# Reactive Geochemical Transport Modeling of Concentrated Aqueous Solutions: Supplement to TOUGHREACT User's Guide for the Pitzer Ion-Interaction Model

Guoxiang Zhang, Nicolas Spycher,
Tianfu Xu, Eric Sonnenthal, and Carl Steefel

**Earth Sciences Division**

**DISCLAIMER**

**ACKNOWLEDGMENTS**

**TABLE OF CONTENTS**

## 1. INTRODUCTION

In this report, we present:

- The Pitzer ion-interaction theory and models
- Input file requirements for using the TOUGHREACT Pitzer ion-interaction model and associated databases
- Run-time error messages
- Verification test cases and application examples.

For the main code structure, features, overall solution methods, description of input/output files for parameters other than those specific to the implemented Pitzer model, and error messages, see the TOUGHREACT User's Guide (Xu et al., 2005).

The TOUGHREACT Pitzer version runs on a DEC-alpha architecture CPU, under OSF1 V5.1, with Compaq Digital Fortran Compiler. The compiler run-time libraries are required for execution as well as compilation. The code also runs on Intel Pentium IV and higher-version CPU-based machines with Compaq Visual Fortran Compiler or Intel Fortran Compiler (integrated with the Microsoft Development Environment).

The minimum hardware configuration should include 1 GB RAM and 1 GB (2 GB recommended) of available disk space.

## 1.1 TOUGHREACT PITZER ION-INTERACTION VERSIONS AND CAPABILITIES

The first version of the nonisothermal reactive geochemical transport simulator, TOUGHREACT, was developed (Xu and Pruess, 1998) by introducing a reactive geochemical model into the framework of the existing multiphase fluid and heat flow code TOUGH2 (Pruess, 1991). TOUGHREACT was further enhanced with the addition of (1) treatment of mineral-water-gas reactive transport under boiling conditions, (2) an improved HKF activity model for aqueous species, (3) gas-species diffusion coefficients calculated as a function of pressure, temperature, and molecular properties, (4) mineral reactive surface area formulations for fractured and porous media, and (5) porosity, permeability, and capillary pressure changes owing to mineral precipitation/dissolution (Sonnenthal et al., 2001; Spycher et al., 2003; Sonnenthal et al., 2005).

The TOUGHREACT versions currently incorporating the Pitzer ion-interaction model described in this document include the Yucca Mountain (YM) versions YM v3.2 and above, and upcoming released (R) versions R v2.0 and above. These Pitzer versions were developed based on the previous versions of TOUGHREACT. The main extensions include (1) the implementation of the Pitzer ion-interaction model (Pitzer and Mayorga, 1973; Pitzer, 1991) for ionic activity calculation of solutions over a broad range of concentrations; (2) the coupling of the vapor-pressure-lowering effect of salinity to phase partitioning; (3) the capability to compute diffusive and advective transport of very small gas amounts (such as acid gases); and (4) a localized iterative algorithm (LIA) for simulation of rapid dryout processes by heating (YM v3.3 only).

Concentrated aqueous solutions are significantly different from dilute solutions not only in terms of geochemical behavior (e.g., water activity and ionic activity coefficients far from unity), but also in terms of flow and transport because of elevated density and viscosity. It should be noted that the Pitzer ion-interaction model implemented in TOUGHREACT is currently used for the calculation of water activity and activity coefficients of dissolved species, but not for other physical properties such as density and viscosity, which are currently assumed to depend only on temperature and pressure.

The Pitzer formalism was implemented into TOUGHREACT using the Harvie-Moller-Weare (HMW) formulation (Harvie et al. 1984) and ion-interaction parameters compiled and updated by Wolery et al. (2004) (see also Alai et al., 2005). The HMW formulation was developed from Pitzer's ion-interaction theoretical model and is equivalent to Pitzer's original model (Pitzer, 1973; and Pitzer and Mayorga, 1973). The only difference is in the definition of interaction terms, interaction coefficients, and mathematical expressions (Rard and Wijesinghe, 2003). The HMW formulation is often preferred to Pitzer's original formulation because it is more convenient for numerical implementation. Also, parameters for the HMW formulation are often more readily available from the literature than parameters for Pitzer's original formulation.

The HMW formulation implemented in TOUGHREACT is documented in APPENDIX A. The implementation of the Pitzer model allows TOUGHREACT to deal with concentrated solutions, with limits on ionic strength, temperature, and pressure depending on the types and validity range of ion-interaction parameters in the thermodynamic database. The current thermodynamic database (after Wolery et al., 2004; see also Alai et al., 2005) is suitable for ionic strengths up to ~40 molal for some systems below 150°C at solution vapor saturation pressures, and is primarily intended for applications involving evaporative concentration at or below ~100°C. The Pitzer model in TOUGHREACT accounts for interaction terms of cation-anion, cation-neutral, anion-neutral, cation-cation, anion-anion, cation-anion-anion, cation-cation-anion, neutral-cation-anion, neutral-cation-cation and neutral-anion-anion combinations (Appendix A). When dealing with reactive transport problems for a given solution, with a pre-estimated ionic strength range, simplifications may be made by neglecting some of these interaction terms to save significant computational time without losing accuracy (Section A.2).

Water activity is a function of concentrations and is significantly lowered in concentrated solutions. Thus, water vapor pressure over such solutions is also lowered, owing to the equilibrium between the solution and its vapor. The lowered vapor pressure can significantly alter vapor flow patterns in a particular system. The lowered vapor pressure also implies elevation of the boiling point. Boiling point elevation alters the temperature field and liquid saturation pattern when a system is heated and solutions are concentrated, thus affecting geochemical processes. The Pitzer model implemented in TOUGHREACT allows the water activity of concentrated solutions to be accurately calculated, such that vapor-pressure lowering, and its subsequent effects, can be properly simulated.

The fugacities (and partial pressures) of volatile gases such as HCl, HF, and $HNO_3$ over dilute solutions are generally quite low at low temperatures (typically $< 10^{-15}$ bar). However, when these solutions become heated and highly concentrated, the fugacities of these gases increase significantly. The fugacities of these gases over highly concentrated solutions can be calculated using the Pitzer model. However, computing the diffusive and advective transport of these gases

over a wide range of partial pressures (typically from $<10^{-15}$ bar to $\sim 10^{-3}$ bar for evaporation/boiling problems at atmospheric pressure and $\sim 100°C$) can create numerical problems because some of the partial pressure values are below machine precision. This problem is solved using an algorithm in which the partial pressures are linearly normalized before transport is computed, then recovered after transport.

In numerical simulations of boiling or evaporation under rapidly drying conditions, a model gridblock can "dry out" between two sequential time steps (i.e., evolve from partially wet to dry conditions, with liquid saturation sharply dropping from a non-zero value to zero or almost zero). In this case, capturing the rapid chemical evolution of the drying solution is important for predicting the precipitation sequence of solid phases, the accompanying gas volatilization, and the composition of the remaining brine. Modeling such a rapid process is extremely challenging. We have therefore developed a localized iterative algorithm (LIA) that gradually removes water from drying model gridblocks until the water activity of the remaining brine reaches equilibrium with the prevailing air relative humidity (i.e., until equilibrium is established between the brine and the vapor phase in contact with it). The LIA enables TOUGHREACT to deal locally with rapid drying processes in simulations that involve otherwise much larger time frames to accurately predict the evolution of the aqueous, solid, and gas phases upon evaporation. The LIA is invoked if (1) the temperature is higher, or equal to, the boiling point, and (2) the water activity is higher than the prevailing air relative humidity (such that the water can be concentrated and thus its activity lowered until equilibrium is reached at the prevailing relative humidity).

## 1.2    CONCENTRATED AQUEOUS SOLUTIONS

Concentrated aqueous solutions are typically defined as aqueous solutions with an ionic strength higher than 1 molal. However, some nonidealities (e.g., nonlinear changes in solution density; Dougherty, 2001) can become significant at ionic strengths as low as 0.1 molal. Concentrated solutions are produced by many natural and artificial processes. Examples include water evaporation/boiling issues with nuclear waste disposal (Alai et al., 2005), seawater intrusion (Harvie and Weare, 1980; Harvie et al., 1984; Krumgalz, 2001), leakage of toxic solutions and electrolytic fluids from storage tanks (Lichtner et al., 2001 and 2004; Steefel et al., 2003; Zhang et al., 2005), and acid mine drainage (Blowes et al., 1991). The mathematical and numerical description of the nonidealities of concentrated aqueous solutions involves many nonlinear ion-interaction terms and various interaction parameter sets (e.g., Pitzer and Mayorga, 1973; Pitzer, 1991; Harvie et al., 1984; Wolery et al., 2004). Thus, numerically modeling these solutions remains a challenge.

Some examples of challenging geochemical systems involving concentrated solutions include those at the U.S. Department of Energy's (DOE) Hanford site (Richland, Washington) and the proposed underground nuclear waste repository at Yucca Mountain, Nevada. At Hanford, a significant amount of high-concentration (up to 10 m and higher – Lichtner and Felmy, 2003) radioactive waste fluids have leaked from underground tanks, leading to contamination of the local groundwater system. At Yucca Mountain, modeling studies indicate that moisture in waste emplacement tunnels and near-field rock pore-water will be boiled and driven away when heat is released from waste packages through radioactive decay. This process will lead to salt precipitation and dryness around the waste-emplacement tunnels. After peak temperatures have

passed, moisture will return into the tunnels and deliquesce the previously precipitated salts. Seepage could also take place within the tunnels during this cooling period and wet the previously deposited salts. Studying fluid migration under these conditions requires a special numerical modeling effort, capturing the effects of ion interactions in concentrated aqueous solutions.

## 2. NEW PROCESS MODELS

## 2.1 PITZER ION-INTERACTION MODEL

In a given aqueous solution, the thermodynamic activity of a dissolved species is a function of the solution excess free energy ─ which is, in turn, a function of temperature, pressure, chemical composition of the solution, and the thermodynamic properties of the solutes. In the solution, ions with opposite signs attract and interact with each other. Some of the ions with opposite signs are bound by their ionic charges, leading to aqueous complexes. Meanwhile, some of the ions tend to depart from each other, leading to the existence of free ions in the solution. The ratio of the bounded ions and free ions is a constant under given composition, temperature and pressure conditions, and is quantified in the thermodynamic equilibrium theory. The thermodynamic activity of any ion in the attraction-repulsion processes is determined by (1) the abundance of that ion in the solution and (2) the nonideal behavior of the ion in solution. The abundance of that ion is the concentration of the free ion. Nonideality, evaluated using an ionic activity coefficient, is a complex function of temperature, pressure, and concentrations.

Dilute solutions (typically with ionic strength, $I$, < 0.1 molal) are considered quasi-ideal solutions. The nonidealities of such solutions are minor and are mainly attributed to long-distance ionic interactions, which can be quantified using ionic strength. The activity coefficients of species in those solutions can be calculated with simple models, such as the Debye-Hückel model and its variations, in which only solution ionic strength and ionic properties are accounted for in the calculation. The effects of interactions among individual ions are neglected.

The nonidealities in concentrated solutions (ionic strength $I$ > 0.1 molal, and especially $I$ > 1 molal) are significant because the distances between ions are much shorter than those in dilute solutions. Most ions in such solutions are neither completely dissociated nor tightly associated, because of the short distance and strong interactions among ions in the solutions. Instead, ions engage in attraction-repulsion interactions with other ions. Ionic activity is mainly attributed to such interactions. Activity models that apply to dilute solutions, such as the Debye-Hückel model and its extensions, are no longer suitable in such concentrated solutions. To calculate ionic activities, one needs to consider interactions among different individual ions.

A quantitative description of how ion interactions affect the ionic activities in concentrated aqueous solutions is given in Pitzer (1973). Pitzer's model formulates the ionic activity as a function of each individual ionic interaction, i.e., the interactions among each cation-anion pair, cation-cation pair, anion-anion pair, and various ternary ionic combinations and other possible interactions. Like-sign pairs and ternary ionic combinations result from multiple salt contributions (also referred to as mixing terms). The Pitzer model evaluates the ionic activity of a solution as a function of solution ionic strength (long-distance interaction), interaction terms (short-distance interaction), temperature, and pressure. The model formulation consists of several

virial equations, sometimes called specific interaction equations, Pitzer equations, or phenomenological equations. These equations can adequately express the thermodynamic properties of the concentrated solution over a wide range of concentrations and temperatures (Clegg and Whitfield, 1991). The Pitzer model is based on a virial expansion (Pitzer, 1973) that essentially reduces to the Debye-Hückel equation at low ionic strength (Pitzer, 1991). This virial expansion involves summations over all possible binary and ternary short-range interaction terms, as well as mixing terms. A generally accepted form of the Pitzer model was formulated by Harvie et al. (1984) and referred to as the HMW formulation. This formulation has been adopted in several computer codes, such as PHRQPITZ (Plummer et al., 1988), GMIN (Felmy, 1995), and BIO-CORE$^{2D\copyright}$ (Zhang, 2001; Zhang et al., 2005). In EQ3/6, Wolery and Daveler (1992) and Wolery and Jarek (2003) use Pitzer's original formulation but also make use of interaction parameters for the HMW formulation by mapping these parameters into the formulation implemented in the code. The HMW formulation was implemented in TOUGHREACT, with details given in Appendix A.

## 2.2    VAPOR-PRESSURE LOWERING

### 2.2.1    Salt Effects

Vapor-pressure lowering caused by dissolved salts was implemented in TOUGHREACT for multiphase flow simulation, using the water activity computed with the Pitzer ion-interaction model (Section 2.1).  For equilibrium between water and $H_2O$ vapor (i.e., for the reaction $H_2O_{(l)} \Leftrightarrow H_2O_{(g)}$), equating the chemical potentials of both phases yields:

$$\mu^0_v - \mu^0_w = RT \ln(f_v/f^0_v) - RT \ln(f_w/f^0_w)$$
$$= RT \ln(f_v/a_w) = RT \ln(K) \tag{2.1}$$

where subscripts $w$ and $v$ stand for liquid water and $H_2O$ gas, respectively, $\mu^0$ stands for the reference chemical potential, $f$ is fugacity, $a$ is activity (defined as $f/f^0$, with $f^0$ being the fugacity in the reference state), $K$ is the thermodynamic equilibrium constant, $R$ is the gas constant, and $T$ is absolute temperature.  The reference (standard) state of $H_2O$ gas is taken as unit fugacity or the pure gas at 1 bar pressure and all temperatures (i.e., $f^0_v$ = 1 bar in Equation 2.1), whereas that of liquid water is taken as unit activity of pure water at all temperatures and pressures (i.e., $f_w/f^0_w = a_w = 1$ in Equation 2.1).  Using this convention yields:

$$f_v = a_w K \tag{2.2}$$

In our case, at low pressure (atmospheric), fugacity is approximated by pressure, such that $f_v \cong P_v$, the pressure of $H_2O$ gas (the actual vapor pressure).  When the system is pure, $a_w = 1$ and Equation (2.2) yields $f_v = K \cong P^0_{sat}$, the vapor pressure of pure water. Accordingly, the vapor pressure of the solution can be computed as:

$$P_v = a_w P^0_{sat} \tag{2.3}$$

Equation (2.3) is used in the coupling of chemistry and flow calculations, such that the effect of salts on vapor pressure is taken into account in the multiphase flow computations. From Equation (2.3), it is also apparent that if relative humidity, $Rh$, is defined as the ratio of the actual vapor pressure over that of pure water, then we have:

$$Rh = a_w \qquad (2.4)$$

### 2.2.2    Salt and Capillary Pressure Effects

The effect of capillary suction on vapor pressure is already included in module EOS4 using a dimensionless modification factor, $F_v$, derived from the Kelvin equation and defined as:

$$F_v = e^{\frac{P_c V_l}{RT}} \qquad (2.5)$$

where $P_c$ is the capillary pressure (Pa), $V_l$ is the molal volume of pure water (m$^3$/mol) at absolute temperature $T$ (in K) and at saturation pressure of pure water, and $R$ is the universal gas constant (Pa m$^3$ mol$^{-1}$ K$^{-1}$).  This factor is used to lower the water vapor pressure as follows:

$$P_v = F_v P^0_{sat} \qquad (2.6)$$

As mentioned above, the standard state for water-activity calculations in TOUGHREACT is unit activity at any temperature and pressure (including negative pressures reflecting capillarity). Using this convention, the effect of capillarity on water activity should be accounted for by the effect of pressure on $K$ in Equation (2.2), without recourse to a separate vapor-pressure-lowering factor, $F_v$ (i.e., by applying a Poynting correction, which is essentially identical to $F_v$, directly to $K$ in Equation 2.2).  However, the water/vapor equilibrium in TOUGHREACT is handled through steam tables for pure water implemented in the TOUGH2 routines of this code, and not through the intermediary of Equation (2.2).  Therefore, Equations (2.3) and (2.4) are valid only when the capillary pressure is zero.  To consider the effect of capillary pressure, these equations need to be replaced by, respectively,

$$P_v = a_w F_v P^0_{sat} \qquad (2.7)$$

and

$$Rh = a_w \times F_v \qquad (2.8)$$

### 2.2.3    Water-Vapor Local Equilibrium

In a groundwater flow system, under typical flow conditions, local equilibrium (water-vapor steady-state system) is generally reached because the groundwater and vapor fluxes are small relative to the rate of local water-vapor transfer.  This local equilibrium is the basic assumption of the TOUGH2 and TOUGHREACT code for multiphase flow calculations.  Local water-vapor equilibrium is always imposed during each flow time step. Thus, the model gives the equilibrium state at each successive time step. Disequilibrium over a large spatial scale is captured by the spatial discretization, with vapor flow being driven by the vapor-pressure gradient from one model gridblock to the next.  Because water-vapor equilibrium is assumed in each gridblock, the

air relative humidity is always 1 if pure liquid water is present and if effects of capillary pressure are neglected.

### 2.2.4 Modified Equation of State (EOS) Modules

The existing modules EOS1, EOS3 and EOS4 of TOUGHREACT were modified to account for salinity-driven vapor-pressure-lowering effects as follows:

- EOS1p and EOS3p: vapor-pressure lowering by salinity only (Equations 2.3 and 2.4)

- EOS4p: vapor-pressure lowering by capillary pressure and salinity (Equations 2.7 and 2.8)

These represent the three EOS modules currently available with the Pitzer version of TOUGHREACT for concentrated solutions.


## 2.3 EVAPORATION/BOILING TO "DRYNESS"

### 2.3.1 Drying, Wetting, and Dryout

For a pure water-vapor system ($H_2O_{(l)} \Leftrightarrow H_2O_{(g)}$) the vapor pressure (i.e., the equilibrium pressure at saturation) is a function of temperature only. When liquid water is in contact with air, evaporation occurs when the partial pressure of $H_2O_{(g)}$ in the air is lower than the water vapor pressure at the prevailing temperature. Here, this case is referred to as "drying": water transfers from the liquid to the gas phase to compensate for the pressure gradient that builds up from the liquid water surface to the air above it. The rate of evaporation is determined by the gradient of $H_2O_{(g)}$ partial pressure at the water surface and the vapor-flow constraints (diffusion and advection). Boiling also occurs when the ambient pressure becomes lower than, or equal to, the water vapor pressure. Conversely, condensation occurs when the partial pressure of $H_2O_{(g)}$ in the air exceeds the water vapor pressure at the prevailing temperature. Here, this case is referred to as "wetting". As in the drying case, the rate of condensation is also determined by the $H_2O_{(g)}$ partial pressure gradient at the water surface and the constraints on vapor flow.

At a given temperature and pressure, under continued drying conditions, pure water will eventually completely vaporize. If, in the process of drying, enough water is transferred from the liquid to the gas phase such that the $H_2O_{(g)}$ partial pressure reaches the water vapor pressure, two-phase conditions remain and thus liquid water and vapor still coexist.

There is rarely any pure water existing in a natural system. Any impurity in water, no matter how dilute the water is, gets concentrated as water is vaporized under drying conditions, potentially leading to concentrated aqueous solutions (i.e., a brine-solid salt-vapor system or a brine-vapor system). As an aqueous solution is concentrated, the water activity and solution vapor pressure are lowered (Equation 2.3). If a solution is put in contact with air having an initial relative humidity < 1, evaporation can proceed only as long as the water activity remains above the air relative humidity (Figure 2-1). The point where equilibrium is reached, when the water activity in the solution (brine) equals the air relative humidity, implies a status of minimum dryness and is referred to, here, as the "dryout point" ("D point" in Figure 2-1). The process leading to

"dryout" is not instantaneous, as constraints on vapor advective and diffusive fluxes dictate the time required for the dilute water to become "dry".
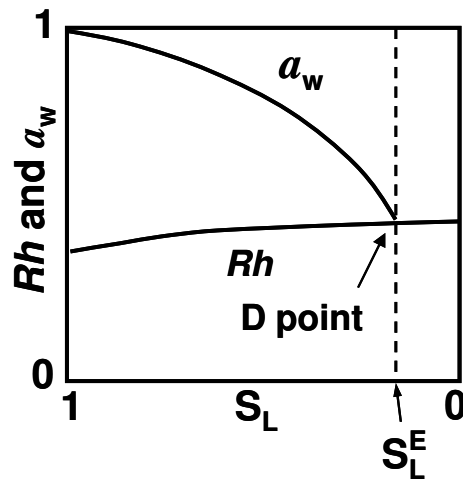


Figure 2-1. Schematic diagram showing the evolution of water activity ($a_w$) and air relative humidity ($Rh$) as a function of water content ($S_L$) upon instantaneous contact of dilute water with air having an initial relative humidity ($Rh$) less than 1. The "dryout" point (D point) is defined as the point at which evaporation cannot proceed further (when $Rh = a_w$, at which point the water content is $S_L^E$).

### 2.3.2    Localized Iteration Approach (LIA) for Simulation of Dryout Processes

As water in a model gridblock evaporates or boils, the concentrations of dissolved components in this gridblock can drastically increase in a single time step. However, the amount of vapor produced (or the absolute amount of water removed) from the boiling concentrated solution gradually become less as the solution is concentrated, because of the vapor-pressure lowering effect. Numerically capturing this drastic change requires very small time steps, typically on the order of $10^{-2}$ seconds or shorter. Therefore, a challenge arises when simulating a spatially large system, with high spatial resolution, over a long simulated time period, because this kind of simulation requires a large number of time steps and gridblocks, thus intensive computation.

Dryout and drastic concentration increases are usually localized (i.e., they take place in a few local areas), with the rest of the modeled domain typically evolving smoothly. For the smoothly changing part of the domain, a very small time step is unnecessary and a waste of computational resources. To capture the localized drying-out processes, a Localized Iteration Approach (LIA) was developed to solve for the equilibrium between final brine water activity and air relative humidity (i.e. the D point in Figure 2-1).

This approach is invoked when a gridblock becomes localized, i.e., the liquid saturation is lower than a prescribed value (typically $S_I < 10^{-4}$ or $S_I < 10^{-5}$) and is boiling or evaporating. In this case, the liquid water flow has almost ceased, the solution is concentrated, and the vapor produced is too small to impact the ambient air relative humidity ($Rh$). At this moment, we describe the water chemistry using $\mathbf{C^0}$, a vector of concentrations:

$$\mathbf{C^0} = (c_1{}^0, c_2{}^0 \bullet\bullet\bullet\bullet\bullet\bullet c_N{}^0)^T \tag{2.9}$$

with a companion vector for a solid-phase (mineral and salts) assemblage:

$$\mathbf{M^0} = (m_1{}^0, m_2{}^0 \bullet\bullet\bullet\bullet\bullet\bullet m_M{}^0)^T \tag{2.10}$$

and a companion vector for the gas assemblage:

$$\mathbf{G^0} = (g_1{}^0, g_2{}^0 \bullet\bullet\bullet\bullet\bullet\bullet g_L{}^0)^T \tag{2.11}$$

where c, m, and g represent concentrations of the solutes in brine, the abundance of minerals and salts, and fugacity (partial pressure) of gases, respectively. Superscripts indicate the boiling/evaporation status (in order of evaporation factor), with 0 denoting the initial stage and D denoting the final stage (i.e., the dryout point), and the subscripts represent the individual components of the system.

At the dryout point, the vectors become:

$$\mathbf{C^D} = (c_1{}^D, c_2{}^D \bullet\bullet\bullet\bullet\bullet\bullet c_N{}^D)^T \tag{2.12}$$

$$\mathbf{M^D} = (m_1{}^D, m_2{}^D \bullet\bullet\bullet\bullet\bullet\bullet m_M{}^D)^T \tag{2.13}$$

$$\mathbf{G^D} = (g_1{}^D, g_2{}^D \bullet\bullet\bullet\bullet\bullet\bullet g_L{}^D)^T \tag{2.14}$$

A big gap in concentrations and partial pressures generally occurs from stage '0' to stage 'D' and, therefore, the geochemical solver may not be capable of reaching stage 'D' in a single simulation step. The LIA was developed for just such situation.

The LIA starts from the initial stage, with $\mathbf{C^0}$, $\mathbf{M^0}$ and $\mathbf{G^0}$ and:

$$a_w{}^0 = F(\mathbf{C^0}) \tag{2.15}$$

where F represents the ensemble of functions that relate the concentrations of aqueous species to the solution water activity (i.e., F embodies the geochemical solver implementing the Pitzer model, including aqueous speciation and mineral/gas reactions). A certain amount of water is then numerically removed from the brine as follows,

$$X_w{}^1 = X_w{}^0 / (1 + \gamma/n^\gamma) \tag{2.16}$$

where $X_w{}^0$ and $X_w{}^1$ represent the water mass (in kg) before and after, respectively, water is removed from the brine (representing one drying iteration), $\gamma$ is a prescribed initial-rate constant for numerically removing water from the brine, and $n$ is the iteration sequence. Usually, a $\gamma$ value of 0.5 or less is used. Equation (2.16) was derived to maximize the convergence of this iterative drying process.

The drying process is thus computed iteratively following the sequence: Initial $\mathbf{C^0}$, $\mathbf{M^0}$, $\mathbf{G^0}$, and $a_w{}^0 \Rightarrow$ Water removal (calculation of $X_w{}^1$ with Equation 2.16) $\Rightarrow$ Calculation of $\mathbf{C^1}$ and $a_w{}^1 = F(\mathbf{C^1})$ (using the existing Newton-Raphson iterative solver for geochemical processes with the Pitzer ionic activity model) $\Rightarrow$ Update of $\mathbf{M}$ (Equation 2.13) and $\mathbf{G}$ (Equation 2.14) $\Rightarrow$ Comparison of $a_w$ with prevailing $Rh \Rightarrow$ Further water removal if $a_w > Rh$, or stop if $a_w \leq Rh$ (i.e. the system has reached the dryout point). This scheme is further depicted in Figure 2-2.
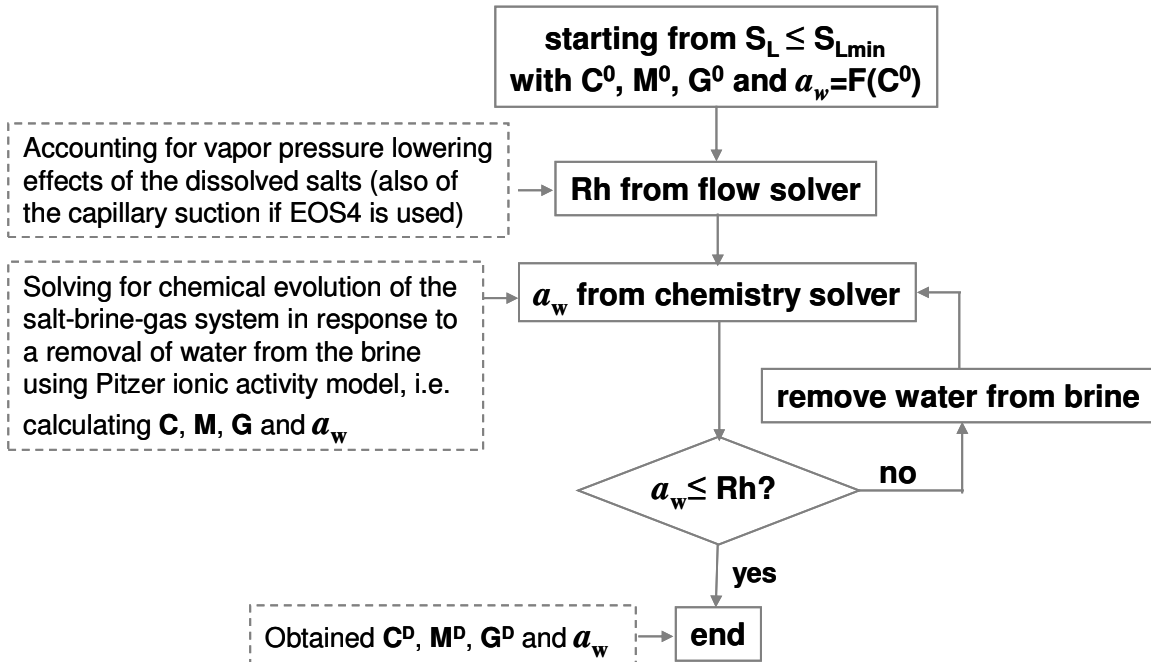


Figure 2-2. Flow chart of the dryout solver (LIA). Abbreviations are the following: $S_L$, liquid saturation; $S_{Lmin}$, prescribed liquid saturation at, and below, which the LIA is implemented; $a_w$, water activity; Rh, relative humidity; $\mathbf{C}$, concentrations; $\mathbf{M}$, mineral abundances; and $\mathbf{G}$, gas partial pressures.

### 2.3.3 Artificially Enhanced Reaction Rates of Minerals While Drying

The rate of boiling/evaporation from the start of the drying-out process (when the liquid saturation is $S_{Lmin}$, Figure 2-2) to the dryout point is generally extremely high. For this reason, it is desirable, in some cases, to artificially enhance the reaction rate of certain minerals during the LIA computations, to ensure their full precipitation (and/or dissolution) in situations when boiling/evaporation rates largely exceed kinetic reaction rates. This is accomplished as described below.

The kinetic precipitation (or dissolution) rate for minerals in TOUGHREACT is described by:

$$r = kA(1 - \Omega^\theta)^\eta \qquad (2.17)$$

10

where $r$ is the rate, $k$ is the rate constant, $A$ is the specific reactive surface area, $\Omega$ is the mineral saturation ratio (the ion activity product Q divided by the solubility product K), and $\theta$ and $\eta$ are two constants specific to each mineral. To increase $r$ during dryout, parameters $\theta$ and $\eta$ in Equation (2.17) are modified as:

$$\theta^{'} = 100\ \theta\ f\ /\ m_w \tag{2.18}$$

and

$$\eta^{'} = \begin{cases} 1 & (\eta < 1) \\ \eta & (\eta \geq 1) \end{cases} \tag{2.19}$$

where $m_v$ is the molecular weight of the mineral, and $f$ is a user-specified constant ranging from 1 to 98. The term $100/m_w$ is introduced here as an arbitrary factor proportional to the unit-formula size of the mineral. Because $\Omega$ is an extensive property, the amplification of $\theta$ would have a disproportionate effect for minerals with large structural formulae (such as clays), compared to simpler minerals (such as quartz), if this factor was not weighted with a unit-formula-dependent parameter.

Note that Equations (2.18) and (2.19), for kinetic-rate amplification, are empirical numerical manipulations to facilitate the precipitation (or dissolution) of minerals reacting under kinetic constraints. The user should have some knowledge of the precipitation sequence of minerals under dryout conditions to apply this option in an appropriate fashion.

## 3.    INPUT FILE UPDATES

### 3.1    UPDATES IN FLOW INPUT (*flow.inp* FILE)

The only updates in file *flow.inp* for using the Pitzer ion-interaction model are in the MOPR parameters, which are input under the keyword "REACT". Parameters MOPR(1) to MOPR(8) are control flags for reactive transport that have not been changed from previous versions (see Xu et al., 2005) and are not described here. Parameters MOPR(9)-MOPR(17) are control parameters for the Pizter ion-interaction model and are described below.

**REACT block          Parameter choices for reactive transport simulation**

> Variable: MOPR(20)
> Format:    20I1

> MOPR(9)    = 0: Forces the code to run with the HKF extended Debye-Hückel activity coefficient model (same model as in previous code versions).
> = 1: **For debugging purposes only!** The code switches between the HKF extended Debye-Hückel model and the Pitzer Model according to a prescribed threshold value of ionic strength that is assigned in *solute.inp* file (see **Record_3** of the *solute.inp* file). This option does not maintain secondary species consistency (see Section 2.5) or

continuity with ionic strength between the two activity coefficient models.

= 2: Forces the code to run with the Pitzer activity coefficient model (HMW formulation).

The default value is 0. See Section 2 for important considerations regarding the compatibility of these two different activity coefficient models, with secondary species included in thermodynamic databases or specified in the *chemical.inp* file.

MOPR(10) and MOPR(11) control the simplification level for the HMW formulation implemented in the code. MOPR(10) takes the value of 0, 1, 2, or 3. MOPR(11) takes the value of 0 or 1. See Appendix A for details on the formulation simplifications corresponding to these options.

MOPR(10)    =  0: no simplification (see Section A.2)
            = 1: neutral-cation-anion terms are omitted.
            = 2: neutral-cation-anion, cation-cation-anion, and cation-anion-anion terms are omitted.

            = 3: neutral-cation-anion, cation-cation-anion, cation-anion-anion, cation-cation, and anion-anion terms are omitted.

MOPR (11)   = 0: ionic strength dependence of the mixing terms is considered.
            = 1: ionic strength dependence of the mixing terms is neglected.

Default values for MOPR(10) and MOPR(11) are 0.  It is the responsibility of the user to ensure that the selected level of simplification is appropriate for the intended use (Appendix A, Section A.2). Typical values for MOPR(10) and MOPR(11) are as follows:

For I < 5 m              MOPR (10) = 3 and MOPR (11) = 1
For I = 5–10 m           MOPR (10) = 2 and MOPR (11) = 0
For I > 10 m             MOPR (10) = 1 or 0, and MOPR (11) =0

MOPR (12)   Together with MOPR (9), MOPR (12) controls the use of thermodynamic databases.  See Section 2 for important considerations regarding the compatibility of the two different activity coefficient models (extended HKF Debye-Hückel and Pitzer) with secondary species included in thermodynamic databases or specified in the *chemical.inp* file. The default value of MOPR (12) is 0.

Use of the extended HKF Debye-Hückel model:

MOPR (9) = 0 and MOPR (12) ≠ 2: the code reads all needed data from the standard TOUGHREACT-formatted thermodynamic database (the file name is specified in the *solute.inp* file).  Note that with TOUGHREACT version YM v3.2 and above, regression coefficients for log(K)'s as a

function of temperature are no longer read from that database (they are skipped on input, and the code performs a regression from the given log(K) values at different temperatures during run time).

MOPR (9) = 0 and MOPR (12) = 2: the code reads primary species, stoichiometries for secondary species, minerals, and gases, as well as all log(K) values from the Pitzer thermodynamic database in EQ3/6-format (skipping over the Pitzer ion-interaction data). The code then reads the standard TOUGHREACT-formatted database for Debye-Hückel activity coefficient data and other data not available in the Pitzer database, such as molecular diameter of gases and molar volume of minerals. The name of the EQ3/6 Pitzer database is by default *data0.ypf*, but a different name can be specified in **Record_4** of the *solute.inp* file, as specified later in this document. This option is generally not used and is intended only to ease comparisons between results using the two available activity coefficient models.

Use of the Pitzer Ion-Interaction Model:

MOPR (9) = 2 and MOPR (12) = 0: the code reads primary species, stoichiometries for secondary species, minerals, and gases, as well as all log(K) values from the standard TOUGHREACT-formatted thermodynamic database, then reads the Pitzer database only for ion-interaction parameters. When using this option, users should manually select secondary aqueous species, if any, consistent with the Pitzer model and input the names of these species in the *chemical.inp* file, making sure that secondary species (ion pairs) already accounted for by the Pitzer ion-interaction parameters are omitted. This will ensure that effects of ion pairs are not "double-counted". See Section 3.3 for important considerations regarding this matter.

MOPR (9) = 2 and MOPR(12) ≠ 0: The code first reads the Pitzer thermodynamic database (in EQ36-format) for all data contained in that database (ion-interaction parameters, primary species, stoichiometries and log(K) values for secondary species and minerals). The code then also reads the standard TOUGHREACT-formatted database, but only for those data that are not in the Pitzer database (molar volume of minerals and molecular diameter of gases).

MOPR(13)     allows the code to read a Pitzer ion-interaction database that is not in EQ3/6-format (and not provided with this package). The default value of MOPR(13) is 0.

MOPR(13) = 0 ALWAYS USE THIS OPTION.

MOPR(13) ≠ 0: the Pitzer thermodynamic database is not in EQ3/6 format. DO NOT USE — for purposes of debugging or parameter development only.

MOPR(14)    This flag is used to enable water vapor-pressure lowering due to dissolved salts (not to be confused with vapor-pressure lowering due to capillary pressure, which is enabled by using the EOS4 module; in that case, the salt effect on vapor pressure is added to the capillary pressure effect).

MOP(14) = 0: vapor-pressure lowering is neglected.
MOP(14) = 1: vapor-pressure lowering is enabled.

Default value is 0. Note that vapor-pressure lowering due to dissolved salts can become quite large at high salinities. To determine whether to consider or neglect this effect, the vapor-pressure lowering factor can be approximated as the water mole fraction in solution (on the basis of fully ionized salts).

MOPR(15)    Place holder (skipped on input; leave blank or non-blank).

MOPR(16)    Place holder (skipped on input; leave blank or non-blank).

MOPR(17)    This flag is used to activate the localized iteration approach (LIA) for solving the dryout processes when a gridblock liquid saturation drops from a value higher than Sl1min (defined in file *solute.inp*) to zero within one time step. In such a case, LIA is used to gradually remove the water from the gridblock and calculate the evolution of solution composition, precipitates, and gases upon evaporation, until the water activity of the residual brine reaches equilibrium with the relative humidity of the air in that gridblock (D point).

MOPR(17) = 0: Localized dryout simulation is inactivated, and the types and amounts of salts precipitated during dryout are calculated using a normative method, as with previous code versions.

MOPR(17) = 1: Localized dryout simulation is activated.

The default value is 0. Note that the precipitation/dissolution rate of kinetically controlled minerals during localized dryout can be either ignored, unchanged, or enlarged by assigning a value to new flag M1 (for kinetically controlled minerals) in **Record-9-1, mineral record 1** of the *chemical.inp* file, as follows:

M1 = −1, rate of the kinetic mineral is 0.
M1 = 0, rate of the kinetic mineral is unchanged.

M1 = 1−98, the precipitation rate of the kinetic mineral is enlarged by amplifying the exponent $\theta$ in the rate equation (Equation (B.5) in *TOUGHREACT User's Guide*, Xu et al., 2005):

$$r_n = f(c1, c2, ..., c_{N_C}) = \pm K_n A_n \left| 1 - \Omega_n^{\theta} \right|^{\eta} \tag{3.1}$$

The exponents $\theta$ and $\eta$ in the above formulation are modified using an empirical formulation (Equations 2.17 and 2.18).

The default value of M1 is 0.

Note that the M1 flag for minerals reacting at equilibrium is inactive (no effect). The M1 flag functions the same as that described in **Record-9-1, Mineral Record 1** of the *chemical.inp* file when MOPR(17)=0 (see *TOUGHREACT User's Guide*, Xu et al., 2005).

## 3.2    UPDATES IN TRANSPORT INPUT (*SOLUTE.INP* FILE)

## Record_3. Options for Reactive Geochemical Transport (2)

Variable: SL1MIN, D1MIN, STIMAX, CNFACT, STR_THRESHOLD
Format:    5E10.4

The first four parameters are unchanged from previous versions (see Xu et al., 2004).

STR_THRESHOLD is a threshold value of ionic strength, enacted only if MOPR(9)=1.   This option is NOT QUALIFIED and for debugging purposes only. When MOPR(9)=1, activity coefficients are calculated using the Pitzer ion-interaction model if the ionic strength is larger than STR_THRESHOLD, and with the HKF extended Debye-Hückel equation if the ionic strength is less than or equal to STR_THRESHOLD.  Note that between these two activity coefficient models, this option does not maintain secondary species consistency (see Section 3.3) or continuity with ionic strength.

## Record_6. Data Related to Convergence Criteria

Two parameters are added to the end of this record, tol_remove and rate_remove.  Other parameters are unchanged from previous versions (Xu et al., 2005).  This input record and new parameters are described below:

Variable: MAXITPTR, TOLTR, MAXITPCH, TOLCH, MAXITPAD, TOLAD, TOLDC, TOLDR, tol_remove, rate_remove
Format: I5, E10.3, I5, E10.3, I5, E10.3, E10.3, E10.3, E10.3, E10.3

tol_remove:  A number used to define dry gridblocks. If the liquid saturation of a gridblock is lower than SL1MIN* tol_remove, this gridblock is considered dry, and the localized dryout simulation for this gridblock is stopped or skipped. This parameter should take a non-zero value between 1 and 1.0E-30, and normally a value between 1.0E-01 and 1.0E-09 is suggested. Note that tol_remove should be estimated, ensuring that the brine water activity and air relative humidity can be equilibrated before the liquid saturation reaches SL1MIN*tol_remove. Default value is $1.0^{-02}$.

rate_remove:  A prescribed constant for calculating the fraction of water removed from the residual brine in each iteration steps of the LIA solver ($\gamma$ in Equation 2.16). The value of this parameter should be in the range of 0.01–0.6, and a suggested value is 0.5. Default value of this parameter is 0.5.

## 3.3    PITZER THERMODYNAMIC DATABASE

The extended TOUGHREACT can directly use the EQ3/6-formatted database *data0.ypf* (Wolery et al., 2004) for both Pitzer ion-interaction parameters and thermodynamic equilibrium constants. These parameters are temperature-dependent. The previous TOUGHREACT-formatted thermodynamic database is also required to provide mineral molal volumes and gas molecular diameters, in case these data are not available in *data0.ypf*.

The interpolation and extrapolation equations, as a function of temperature, for various thermodynamic properties of aqueous solutions, for binary and ternary systems, and for multiple-component mixtures within the Pitzer formulation have been reported in many papers (Harvie et al., 1984; Pabalan and Pitzer, 1989; Harvie et al., 1987; Moller, 1988; Greenberg and Moller, 1989; Monnin, 1989 and 1994; Pitzer, 1991; Weber et al., 1999). These authors utilized a variety of activity data, enthalpy data, and heat capacities to construct comprehensive equations over the temperature range of 0 to 250$^{o}$C. For example, Pabalan and Pitzer (1989) fitted their experimental results with equations using more than twenty adjustable parameters. Moller (1988) and Greenberg and Moller (1989) used an equation with ten adjustable parameters to describe the temperature-dependent parameters. In the Pitzer version of TOUGHREACT, we use the following algebraic equation from Wolery et al. (2004):

$$P(T) = a_1 + a_2 (\frac{1}{T} - \frac{1}{T_0}) + a_3 \ln(\frac{T}{T_0}) + + a_4 (T - T_0) \qquad (3.2)$$

where *P(T)* represents Pitzer parameters $\beta^{(o)}$, $\beta^{(1)}$, $\beta^{(2)}$, $\alpha$, $\Phi$, $\Psi$, and $C_{MX}^{\Phi}$ at temperature *T* (absolute temperature); and $T_0$ is the reference temperature (298.15 K used in the database). These data are generally good up to at least 90$^{o}$C and were derived specifically for the Yucca Mountain Project. More details on the database can be found in Wolery et al. (2004) and Alai et al. (2005).

The dependency of the Pitzer parameters on pressure is not considered in the present model, because the effect of pressure is much less significant than the effect of temperature within the current temperature range considered.

In addition to the EQ3/6-formatted Pitzer database, the code can also use the regular TOUGHREACT-formatted thermodynamic database and an unformatted database for Pitzer ion-interaction parameters from Zhang et al. (2005). The unformatted database is easy to extend and modify, and could be useful for users who develop their own parameters. Users can read the parameters from either database by simply assigning different option parameters in the input file (MOPR(12), see Section 3.1).

Because the effect of ion pairing and aqueous complexations (forming secondary aqueous species) is generally taken into account by the ion-interaction parameters, much care must be taken to avoid "double counting". Such an occurrence can be avoided by including in simulations only those secondary species that were specifically included in the fits of experimental data used to determine the ion-interaction parameters used in the simulation.

## 4.    RUN-TIME ERROR MESSAGES

In addition to the run-time error messages given in the *TOUGHREACT User's Guide* (Xu et al., 2005), run-time error messages related to the Pitzer model were added to the code and described below.

**From Routine: PITZ_DATA**
      Error opening pitzdata: stop
      Execution stop: yes.  Self-explanatory.

      Error reading positive-negative pairs: stop pitz_data
      Execution stop: yes.  Self-explanatory.

      Error reading neutral-positive pairs: stop pitz_data
      Execution stop: yes.  Self-explanatory.

      Error reading neutral-negative pairs: stop pitz_data
      Execution stop: yes.  Self-explanatory.

## 5.    VERIFICATION TESTS AND SAMPLE PROBLEM

## 5.1    VERIFICATION TESTS

### 5.1.1    Verification Test 1: Calculation of the Mean Activity Coefficients of *CaCl$_2$* and Osmotic Coefficient of Solutions up to 9 m *CaCl$_2$* at Temperatures of 60°C, 80°C, and 100°C

In this test, we calculate the mean activity coefficients of *CaCl$_2$* and the osmotic coefficient of solutions up to 9 molal *CaCl$_2$* at temperatures of 60°C, 80°C, and 100°C, using TOUGHREACT (the EOS3 module; note that this test problem is not relevant to EOS modules).  The calculated

mean $CaCl_2$ activity and osmotic coefficients of the solution are then compared with the data from Ananthaswarmy and Atkinson (1985). These authors collected measured thermodynamic properties of $CaCl_2$ solutions at various temperatures and concentrations (e.g., activity coefficients, osmotic coefficients, apparent mole heat capacity, apparent model enthalpies, differential heat of dilution of $CaCl_2$ in temperature range 0–100$^{\circ}$C, and water-vapor-pressure data), fitted data set to appropriate Pitzer equations as modified for $CaCl_2$ by Rogers (Rogers 1981), and presented the mean activity coefficients, osmotic coefficients for $CaCl_2$ solutions at various temperature and various molalities as reference data of $CaCl_2$ solutions. Note that comparisons of mean activity coefficients, rather than mean activities, are appropriate here, because no significant amounts of $Ca$ or $Cl$ secondary species are calculated to form.

The mean activity coefficient of $CaCl_2$ is calculated as:

$$ln( \gamma_{CaCl_2} ) = \frac{2\,ln( \gamma_{Cl} ) + ln( \gamma_{Ca} )}{3} \qquad (5.1)$$

where $\gamma_{CaCl_2}$ is the mean activity coefficient of $CaCl_2$, $\gamma_{Ca}$ is the activity coefficient of $Ca^{+2}$, and $\gamma_{Cl}$ is the activity coefficient of $Cl^{-}$.

The osmotic coefficient is calculated as:

$$\phi = -\frac{ln( a_w )*1000}{W_w \sum_i m_i} \qquad (5.2)$$

where $\phi$ is solution osmotic coefficient, $a_w$ is water activity (calculated with TOUGHREACT and read from file *chdump.out*), $W_w$ is the water molecular weight, and $m_i$ is the molality of each aqueous species $i$ in the solution. The comparison between the calculation and the reference data is shown in Figure 5-1.

The root-mean-square error (RMSE) of the mean activity coefficient is 10.95% and that of the osmotic coefficient is 3.76%.
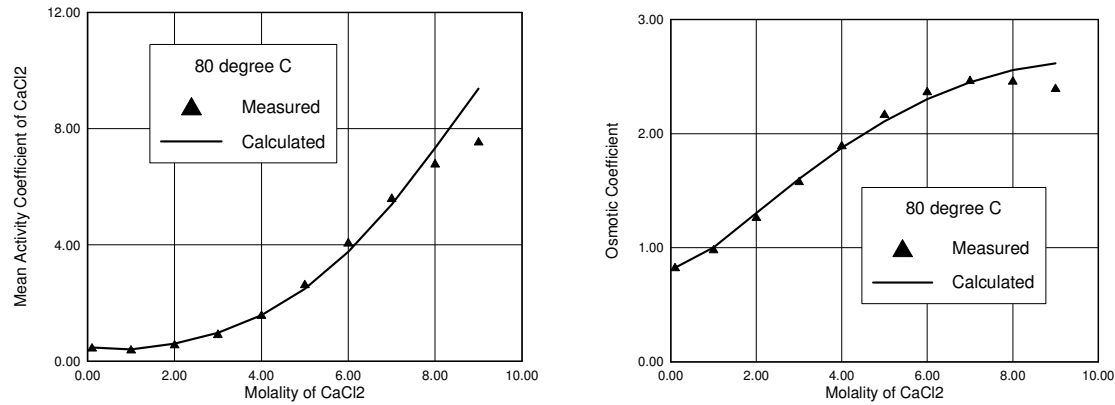
Figure 5-1. Comparison of the TOUGHREACT-calculated (solid lines) mean activity coefficient of *CaCl₂* and osmotic coefficient of the *CaCl₂* solution to literature data (symbols) from Ananthaswarmy and Atkinson (1985).

Note that Ananthaswarmy and Atkinson (1985) report that at high ionic strength, their data are questionable. This may be a result of a possible solid phase formed in the solution at concentrations reaching saturation of the salt. This would explain the larger discrepancies between their data and the TOUGHREACT results at high *CaCl₂* concentrations (Figure 5-1). The results of this test are independent from the selected EOS module, because flow and transport processes are not involved in these computations.

### 5.1.2 Verification Test 2: Calculation of The Mean Activity Coefficients of *NaCl*, and the Osmotic Coefficient of *NaCl* Solutions up to 6 m at 0°C, 25°C, 50°C, 80°C, 100°C, and 110°C, Respectively

This test involves calculating the mean activity coefficients of *NaCl*, and the osmotic coefficient of *NaCl* solutions up to 6 molal of *NaCl* salt, at 0°C, 25°C, 50°C, 80°C, 100°C, and 110°C. The results are compared with data measured by Clarke and Glew (1985). This test case validates the calculated temperature dependency of activity coefficients. Note that comparisons of mean activity coefficients, rather than mean activities, are appropriate here, because no significant amounts of *Na* or *Cl* secondary species are calculated to form. Also, the results of this test are independent of the selected EOS module because flow and transport processes were not considered.

The mean activity coefficient of *NaCl* is calculated with:

$$ln( \gamma_{NaCl} ) = \frac{ln( \gamma_{Cl} ) + ln( \gamma_{Na} )}{2} \tag{5.3}$$

The root-mean-square errors (RMSE) were also calculated and are much smaller than 1% (see Figure 5-2).
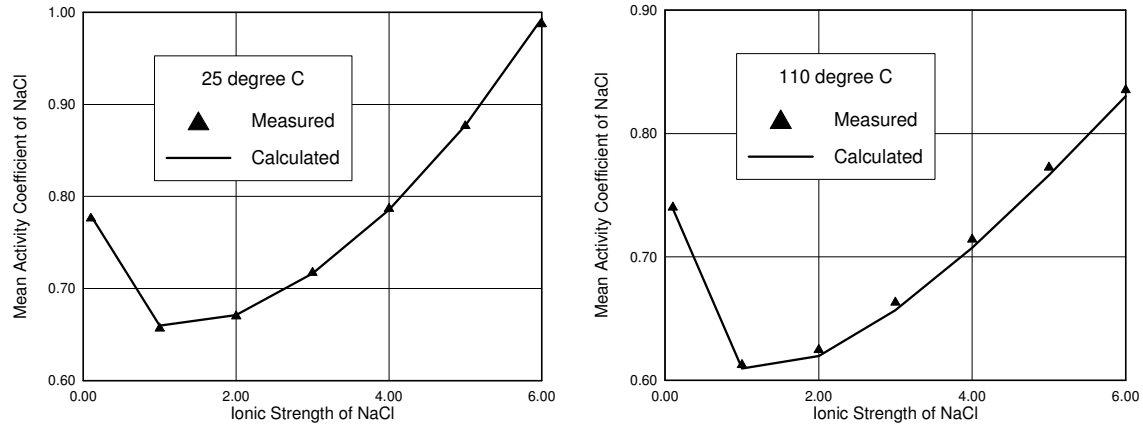
Figure 5-2. Examples of TOUGHREACT-calculated (solid lines) and measured (symbols) mean activity coefficients for NaCl solutions (25$^{o}$C on the left and 110$^{o}$C on the right). Measured data are from Clarke and Glew (1985).

### 5.1.3 Verification Test 3: Calculation of the Water Vapor Pressure over *CaCl$_2$* Solutions at Concentrations up to 9 m at 25$^{o}$C, Using the EOS3 Module

This test involves the calculation of the water vapor pressure over *CaCl$_2$* solutions at concentrations up to 9 m *CaCl$_2$* at 25$^{o}$C, using TOUGHREACT EOS3p. This test verifies the EOS3p capability to take into account vapor-pressure lowering caused by dissolved salts.

To verify the vapor-pressure-lowering effect, the vapor pressure of *CaCl$_2$* solutions up to 9 m *CaCl$_2$* was hand-calculated by taking the vapor pressure of pure water from the NIST steam tables (Wagner and Pruβ, 2002), and then calculating the vapor pressure of the solution, using Equation (2.3), and the water activity calculated by the Pizer ion-interaction model. TOUGHREACT-simulated vapor pressure and relative humidity values for solutions up to 9 m *CaCl$_2$* salt agree well with the values calculated from the steam tables (Figure 5-3).

The TOUGHREACT-simulated vapor pressures are obtained by taking the air mass fraction, $X_{air}$, from output file *flow.out*, and converting into vapor pressure, using:

$$P_v = \frac{(1-X_{air})p_{tot}}{1-(1-\frac{W_w}{W_{air}})X_{air}} \tag{5.4}$$

where $P_v$ is the vapor pressure, $p_{tot}$ is total pressure, $X_{air}$ is mass fraction of air, and $W_w$ (18.061 g/mol) and $W_{air}$ (28.96 g/mol) are the molecular weights of water and air, respectively. $p_{tot}$ and $X_{air}$ are calculated by TOUGHREACT and output in file *flow.out*. Equation (5.4) is derived according to the mass conservation law implemented in EOS3 (where the gas phase consists of air and water vapor only, Pruess et al., 1999).
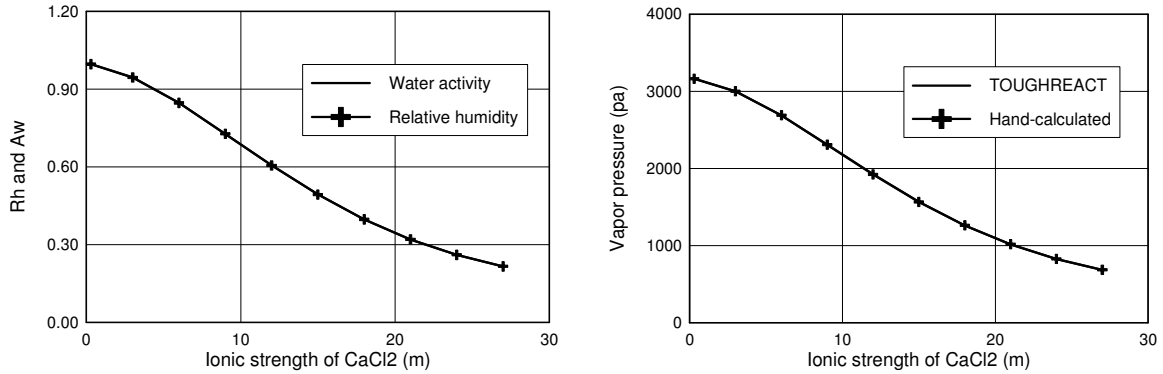
Figure 5-3. Comparison of water activity and relative humidity (left), and comparison of TOUGHREACT-calculated and hand-calculated vapor pressures (right). The relative difference between *Rh* and $a_w$ is much smaller than 1%. The relative difference between the TOUGHREACT-simulated vapor pressure and hand-calculated vapor pressure is also smaller than 1%.

### 5.1.4 Verification Test 4: Calculation of the Water Vapor Pressure over *CaCl₂* Solutions at Concentrations up to 9 m at 25°C, Using the EOS4 Module

This test is the same as Test 3, using EOS4p instead of EOS3p. This test verifies the EOS4p capability to account for vapor-pressure lowering caused by dissolved salts. The vapor pressure over *CaCl₂* solutions at concentrations up to 9 molal of *CaCl₂* and at variable temperatures is calculated using TOUGHREACT EOS4p. In this case, the relative humidity (*Rh*) over a saline solution in a porous medium is reduced by both salinity and capillary suction.

The effect of capillary suction on vapor pressure is calculated in EOS4p as described in Section 2.2.2, using a vapor-pressure-lowering factor ($F_v$) defined with Equation (2.5). This factor (essentially a Poynting correction) was independently calculated using Equation (2.5) and water volume values from the NIST/ASME Steam Tables. The relative humidity values output from TOUGHREACT was then compared with $a_w F_v$ (Equation 2.8), taking the values of $a_w$ from output file *chdump.out*. The vapor pressure ($P_v$) was hand-calculated using Equation (2.7), taking the vapor pressure of pure water at different temperatures ($P^0_v$) from the NIST/ASME Steam Tables and $a_w$ values from output file *chdump.out*. The vapor-pressure values obtained in this way were then compared to the values indirectly computed by TOUGHREACT, obtained by $P_{tot} - P_{air}$, with $P_{tot}$ and $P_{air}$ being the total gas-phase pressure and air pressure output from the code in file *flow.out*. Results are shown in Figure 5-4. The relative differences are smaller than 1%.
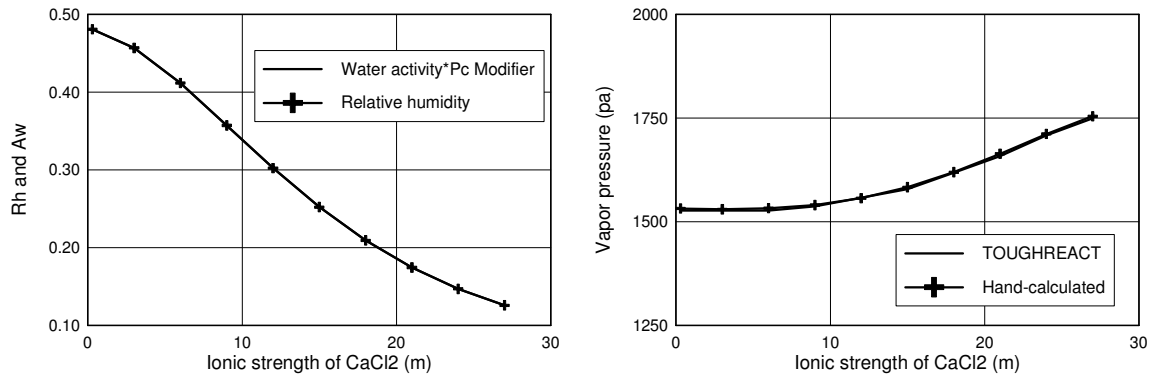
Figure 5-4. Comparison of water activity with relative humidity (left), and comparison of vapor pressures (right)

## 5.2    SAMPLE PROBLEM: MODELING BOILING/CONDENSATION OF A SYNTHETIC YUCCA MOUNTAIN UNSATURATED ZONE PORE WATER

A boiling/condensation experiment using a synthetic concentrated Yucca Mountain unsaturated zone pore water (Sonnenthal and Bodvarsson, 1999) was conducted by Pulvirenti et al. (2004), focusing on the corrosion of Alloy 22 (a Ni-Cr-Mo alloy) placed in an evaporation flask. The experiment was set up as shown in Figure 5-5.
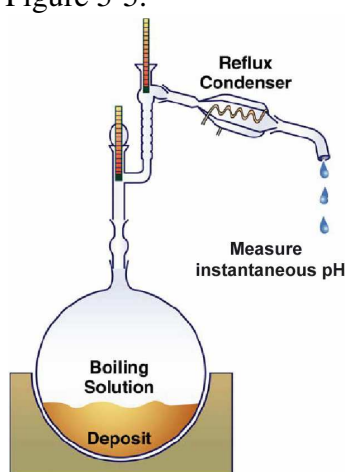


Figure 5-5. Schematic illustration of the evaporation/condensation experiment conducted by Pulvirenti et al. (2004)

Multiple salts were used to synthesize a concentrated solution that may represent a rare type of Yucca Mountain tuff pore water concentrated by 1243 times. The recipe used to synthesize this solution is documented in Pulvirenti et al., (2004). Using this recipe, the resulting chemical composition of the synthetic concentrated pore water was determined and listed in Table 5-1.

Twelve liters of the synthetic concentrated solution was prepared, and distilled in a round-bottom flask within a heating mantle, at 144°C. A water-cooled condenser was attached at the top of the flask. Condensates were collected at intervals for *pH* measurement. As the solution volume in the flask reduces to 40–250 mL, corresponding to a concentration factor in the range 59664–372900 from the pristine Yucca Mountain pore water, the *pH* of the condensed droplets fell to 1 or lower.

Table 5-1. Initial chemical composition of the synthetic concentrated porewater used in the experiment

| Components | Concentration (moles/kg of water) |
|---|---|
| pH | neutral |
| $Ca^{+2}$ | 4.2609E-01 |
| $Cl^-$ | 1.5954E+00 |
| $F^-$ | 3.0940E-02 |
| $HCO_3^-$ | 7.8739E-04 |
| $K^+$ | 7.3828E-02 |
| $Mg^{+2}$ | 2.4910E-01 |
| $Na^+$ | 2.9866E-01 |
| $SO_4^{-2}$ | 2.3678E-02 |
| $SiO_{2(aq)}$ | 1.3088E-05 |
| $NO_3^-$ | 4.5102E-02 |

The setup for the experiment of Pulvirenti et al. (2004) is simply discretized using a number of finite difference blocks, as schemed in Figure 5-6. Initially, the flask is filled with 12 L of the concentrated pore water with chemical composition shown in Table 5-1. A heat load is applied into the flask to boil the solution. The simulation starts from the boiling of the solution (temperature is $100^{\circ}$C). The boiling temperature is then elevated as a function of the solution's ionic strength because of vapor-pressure lowering (Figure 5-7). It is assumed that there are no solid phases initially in contact with the solution (initial solid phases are all zero). The atmosphere is represented by a huge block ($10^{58}$m$^3$) assigned atmospheric physical and chemical properties. The $CO_2$ partial pressure in the atmosphere is $3.55\times10^{-4}$ bar, and that of $HCl$ is $10^{-15}$ bar. The partial pressures of all gases are initially assumed to be in equilibrium with the solution in the beaker, whereas those of $HF$ and $HNO_3$ were assumed to be zero elsewhere. Only the end block (at the condenser outflow) is allowed contact with the atmosphere; other parts of the experimental device are hydraulically closed. Heat loss is accounted for by vapor flow out of the system. Most of the vapor produced discharges into the atmosphere; a minor amount is condensed in the condenser, represented by a cooler block at $25^{\circ}$C (Figure 5-6). Air from the atmosphere block is allowed to diffuse into the flask through the tube, while gases generated in the flask flow out through the tube, and (mostly) dissolve into the condensed water in the condenser, leading to a decrease in the condensate $pH$. The condensed acid water flows out of the tube and drops into the atmosphere block.
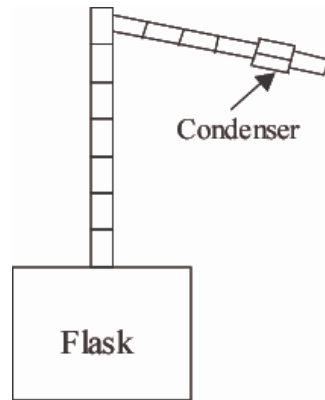
Figure 5-6. Schematic illustration of the finite differential discretization of the boiling/condensation experiment of Pulvirenti et al. (2004). Volumes of the flask is 15 L and the outer diameter of the pipe is assumed to be 1.0 cm and inner diameter is assumed to be0.7 cm.

The solution is initially supersaturated with respect to calcite, which immediately precipitates at the start of the simulation. A number of salts are allowed to precipitate when the solution is further concentrated: *CaCl₂*, *CaCl₂:2H₂O*, *gypsum*, *niter*, *soda niter*, *halite*, *sylvite*, *epsomite*, *Mg(NO₃)₂*, *nahcolite*, *villiaumite*, *carobbite*, and *MgCl₂:4H₂O*.   $CO_2$, $HCl$, $HF$, and $HNO_3$ gases are considered in the simulation as volatilized and diffused into the atmosphere through the pipe as the solution is being concentrated.

The simulated temperature of the boiling solution in the beaker increases as a function of the concentration factor (Figure 5-7), caused by vapor-pressure lowering. The temperature evolution is clearly controlled by the solution chemistry evolution, mostly through the precipitation of salts (Figure 5-8).
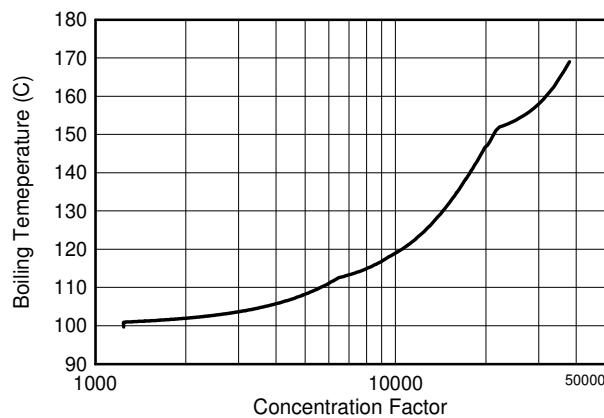


Figure 5-7. Simulated boiling temperature as a function of concentration factor

Figure 5-8 shows the aqueous-concentration evolution trends and the salts precipitated as a function of the concentration factor. Concentrations of all aqueous components increase monotonically before *NaCl* starts to precipitate at a concentration factor of 6500. After that, the Na⁺ concentration decreases, but $Cl^-$ concentration continues to increase, although at a reduced rate, because $Cl^-$ is initially far more enriched than Na⁺. Another significant event controlling the concentration evolution is the precipitation of *CaCl₂:2H₂O*, starting at a concentration factor

of 21,000. The precipitation of this salt removes $Ca^{+2}$ from the solution and causes the decrease of this cation. $Cl^-$ concentration continues to increase but at a further reduced rate. Nitrate salts were not predicted to form, even at the final concentration factor of 38,000. Precipitation of sylvite started at a concentration factor of 9,500, causing the concentration evolution trend to change slightly.
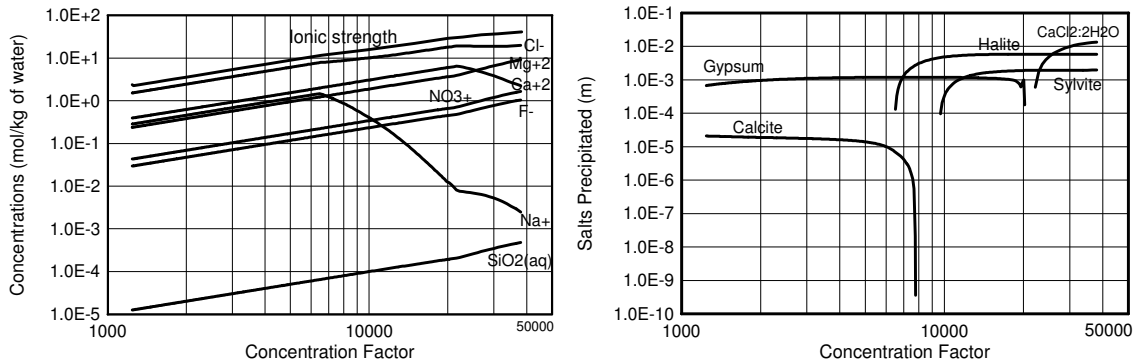


Figure 5-8. Simulated concentrations of aqueous components and the ionic strength of the boiling solution, and salts precipitated (changes of abundance in volume fraction) from the boiling solution as a function of concentration factor.

Three major acid gases, *HCl*, *HF*, and *HNO₃*, are predicted to exsolve from the boiling solution (Figure 5-9). The partial pressures of these gases gently increase before *NaCl* precipitation. After that, partial pressures of these gases increase at a reduced rate, caused by the precipitation of *NaCl* removing *Cl⁻* from the solution. Once *CaCl₂* starts to precipitate, the partial pressures of *HCl*, *HF*, and *HNO₃* are controlled by the precipitation of this salt. Partial pressures of these gases in the condenser increase similarly to the gases in the beaker, but lowered by about 50% of the values in the beaker, because of the pressure gradient induced by transport.
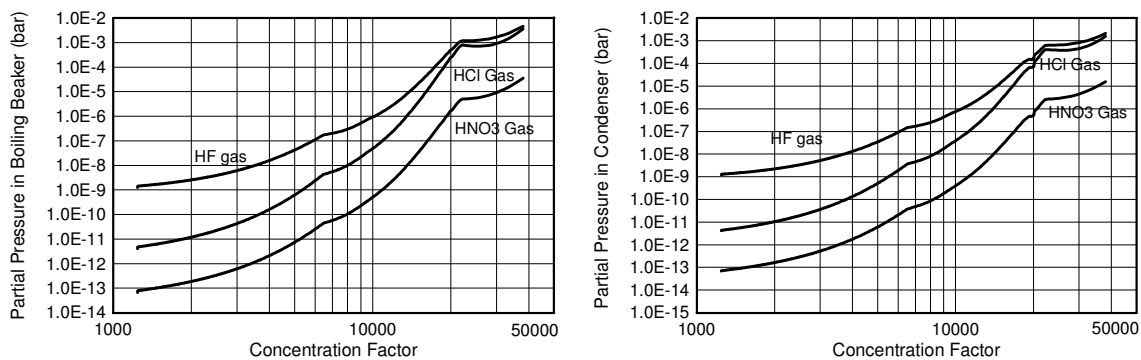


Figure 5-9. Simulated acid gases (partial pressure in bar) generated from the boiling solution (left) and acid gases partial pressure in the condenser (right) as a function of concentration factor

Vapor condenses in the condenser when cooled to 25°C. Acid gases dissolve immediately into the condensed water, causing the *pH* of the condensate to drop. The *pH* of the condensate is controlled by the fugacities of the acid gases and the mass fraction of the water vapor in the gas phase. The less water condenses in the beaker, the lower the *pH* of the condensate.

The simulated *pH* of the boiling solution and the condensate are plotted in Figure 5-10 as functions of the concentration factor. The *pH* of the boiling solution gently decreases,

corresponding to the precipitation of calcite, from 8 to 6.6, until the concentration factor reaches 6,500. Then, the pH is buffered by *NaCl* precipitation. When the concentration factor is greater than 21,000, the starting point of the $CaCl_2:2H_2O$ precipitation, the *pH* is buffered by the salts. The *pH* of the condensate is controlled by the acid gas partial pressure (fugacity) and evolves similarly to the *pH* of the boiling solution. The *pH* of the condensate reaches –1.7 at concentration factor 38,000. Predicted extremely low *pH* values are consistent with experimental observations. However, such low *pH* values occur only when the water vapor mass fraction is smaller than about 2%.
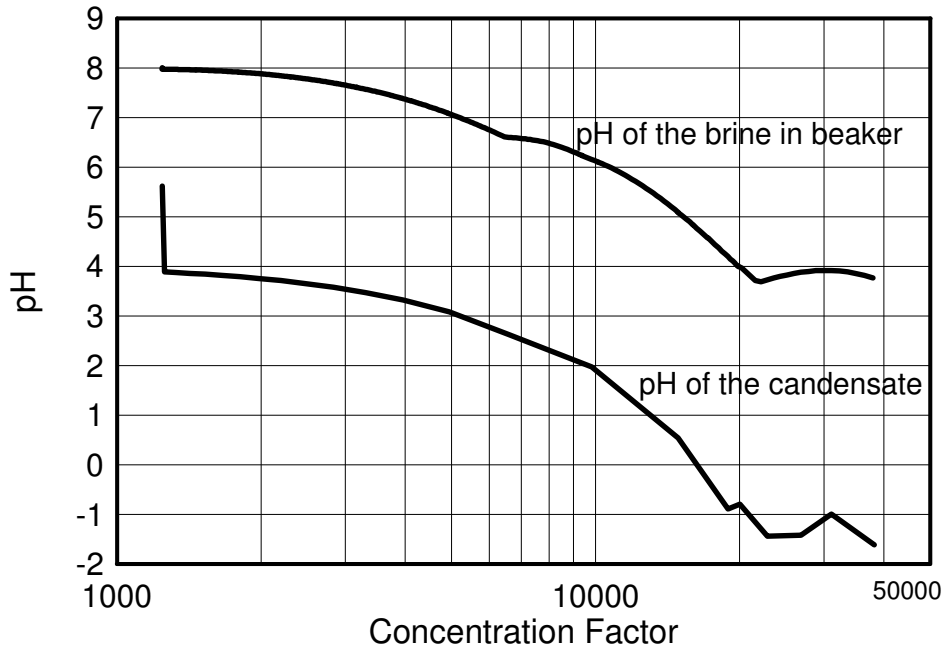


Figure 5-10. Simulated *pH* of the boiling solution and the condensate as a function of the concentration factor

Model results reproduce the measured very low *pH* (<1) of the condensate and confirm the findings of the experiment. The extremely low *pH* appears only when the initial 12 L synthetic concentrated (1243 times) pore water has boiled down to a volume of around 40–250 mL, corresponding to a concentration factor of ~60,000–370,000. The *pH* of the remaining liquid is predicted to be about 3.8. The 12 L synthetic concentrated pore water is equivalent to 14.916 m$^3$ of pristine porewater. When the *pH* of the condensed water droplet reaches <1, more than 99.99% of the equivalent pristine pore water has been vaporized.

The simulation included one boiling event and a number of condensing events. While simulating boiling, the condenser grid block was made inoperative by removing the 25$^o$C temperature constraint, to avoid the accumulations of the condensate in the condenser and continuous scrubbing of water and acid gases. The boiling run was started at a concentration factor 1243 (i.e., the initial concentration factor of the synthetic solution, relative to the pristine pore water) with maximum time step of 5 seconds, run to a concentration factor of 9,739, and then restarted with maximum allowed time step of 0.2 second to capture the rapid boiling processes. TOUGHREACT automatically controls the time steps and reduces the time step as the chemical evolution is becoming faster. The run was finally stopped at a concentration factor of 43,186

where the solution ionic strength reaches 41.7 m. The condensing runs were carried out by restarting the boiling run with the condenser temperature set at 25$^{\circ}$C at specified time intervals (i.e., at different concentration stages), for calculating the instantaneous chemical compositions (including pH) of the condensate.   The results shown in Figure 5-7 through Figure 5-10 for the condenser grid block represent computed compositions with the condenser turned off, except for *pH* in Figure 5-10 which represent the *pH* of condensate cooled to 25°C.

The input files of the boiling run are shown in Figure 5-11 through 5-17.



Figure 5-11.   Part of the TOUGHREACT input file, *flow.inp*, for the sample problem discussed above: Data blocks ROCKS, REACT, PARAM, START and TIMES.

```
File  Edit  Search  View  Tools  Macros  Configure  Window  Help
```

```
ELEME----1----*----2----*----3----*----4----*----5----*----6----*----7----*----8
F00 0           beak 1.5000E-022.5300E-01                         0.000    0.0000
TP0 1           pipe 3.9250E-061.5700E-03                         0.000    0.0500
TP0 2           pipe 3.9250E-061.5700E-03                         0.000    0.1000
TP0 3           pipe 3.9250E-061.5700E-03                         0.000    0.1500
TP0 4           pipe 3.9250E-061.5700E-03                         0.000    0.2000
TP0 5           pipe 3.9250E-061.5700E-03                         0.000    0.2500
TP0 6           pipe 3.9250E-061.5700E-03                         0.000    0.3000
TP0 7           pipe 3.9250E-061.5700E-03                         0.000    0.3500
TP081           pipe 3.9250E-021.5700E-05                         0.000    0.4000
TP0 8           pipe 3.9000E-061.5700E-03                         0.000    0.4000
TP0 0           atmos0.5000E+580.0000E+00                         0.000    0.5000
con 1           air

CONNE
TP0 1F00 0                       10.2500E-010.1550E+007.8500E-050.1000E+01
TP0 2TP0 1                       10.2500E-010.2500E-017.8500E-05-.0700E+01
TP0 3TP0 2                       10.2500E-010.2500E-017.8500E-05-.0700E+01
TP0 4TP0 3                       10.2500E-010.2500E-017.8500E-05-.0700E+01
TP0 5TP0 4                       10.2500E-010.2500E-017.8500E-05-.0700E+01
TP0 6TP0 5                       10.2500E-010.2500E-017.8500E-05-.0700E+01
TP0 7TP0 6                       10.2500E-010.2500E-017.8500E-05-.0700E+01
TP0 8TP0 7                       10.2500E-010.2500E-017.7800E-05-.0700E+01          !
TP081TP0 7                       10.2500E-010.2500E-017.8500E-05-.0700E+01
TP0 0TP081                       10.2500E-010.2500E-017.8500E-05-.0700E+01
TP081TP0 8                       10.2500E-010.2500E-012.6167E-06-.0700E+01
TP0 0TP0 8                       10.1550E+000.2500E-010.1000E+000.1000E+01          !
```

```
flow.inp
```

```
For Help, press F1                        1      1      Read  Ovr  Block  Sync  Rec
```

Figure 5-12.   Part of the TOUGHREACT input file, *flow.inp*, for the sample problem  discussed above: Data block ELEME and CONNE.

Figure 5-13. Part of the TOUGHREACT input file, *flow.inp*, for the sample problem discussed above: Data blocks GENER, INCON and MULTI.

Figure 5-14.  The TOUGHREACT input file, *solute.inp*, for the sample problem discussed above.

```
TextPad - [C:\Share C\cu_experiment_run_for_paper\run13\chemical.inp]
 File  Edit  Search  View  Tools  Macros  Configure  Window  Help

'DEFINITION OF THE GEOCHEMICAL SYSTEM'
'PRIMARY AQUEOUS SPECIES'
'h2o'
'h+'
'ca++'
'cl-'
'f-'
'hco3-'
'k+'
'mg++'
'na+'
'so4--'
'sio2(aq)'
'no3-'
'*'
'MINERALS'
'cacl2'   0 0 0 0
0. 0. 0.
'cacl2:2h2o' 0 0 0 0
0. 0. 0.
'calcite'  0 0 0 0
0. 0. 0.
'gypsum' 0 0 0 0
0. 0. 0.
'niter'  0 0 0 0          !KNO3
0. 0. 0.
'soda niter'  0 0 0 0     !NaNO3
0. 0. 0.
'halite'  0 0 0 0
0. 0. 0.
'sylvite'  0 0 0 0
0. 0. 0.
'epsomite' 0 0 0 0        !MgSO4 7H2O
0. 0. 0.
'mg(no3)2' 0 0 0 0
0. 0. 0.
'nahcolite' 0 0 0 0       !NaHCO3
0. 0. 0.
'villiaumite' 0 0 0 0     !NaF
0. 0. 0.
'carobbite'  0 0 0 0      !KF
0. 0. 0.
'mgcl2:4h2o' 0 0 0 0
0. 0. 0.
'*'                 0.0      0  0 0
'GASES''co2(g)' 0
'co2(g)'
'hcl(g)'
'hf(g)'
'HNO3(g)'
'*'
```

  chemical.inp
File: chemical.inp, 6301 bytes, 141 lines, UNIX, ANSI          1        1    Read Ovr Block Sync Rec Caps

Figure 5-15.  Part of the TOUGHREACT input file, *chemical.inp*, for the sample problem discussed above: chemical components.

Figure 5-16.   Part of the TOUGHREACT input file, *chemical.inp*, of the sample problem discussed above: initial concentrations of the solution components.

File  Edit  Search  View  Tools  Macros  Configure  Window  Help

```
 1
'mineral         vol.frac.        ''cacl2'              0.00000   0
'cacl2'           0.00           0                  !'calcite'           0.00           0
'*'               0.0            0
'-----------------------------------------------------------------------'
'INITIAL gas ZONES'
2                                 !ngtype= number of gas zones
1                                 !igtype
'gas        partial pressure'   !                                         'co2(g)'
'hcl(g)'          0.00
'co2(g)'          0.00
'hf(g)'           0.00
'hno3(g)'         0.00
'*'               0.0
2                                 !igtype 2 atomsphere
'gas        partial pressure'   !                                         'co2(g)'        3.54
'hcl(g)'          1.000e-15
'co2(g)'          3.549e-4
'hf(g)'           0.00
'hno3(g)'         0.00
'*'               0.0
'-----------------------------------------------------------------------'
'Permeability Zones'
 1
 1
'perm law    a-par   b-par tcwM3'
    1    0.0000E+00    0.0000E+00
'-----------------------------------------------------------------------'
'INITIAL SURFACE ADSORPTION ZONES'
0                         !ndtype= number of sorption zones
'zone       ad.surf.(m2/kg)  total ad.sites (mol/l)'
'-------------------------------------if Sden=0 Kd store retardation factor'
'INITIAL LINEAR EQUILIBRIUM Kd ZONE'
1                                 !kdtpye=number of Kd zones
1                                 !idtype
'species    solid-density(Sden,kg/dm**3)  Kd(l/kg=mass/kg solid / mass/l'
'*'               0.0            0.0
'-------------------------------------if Sden=0 Kd store retardation factor'
'INITIAL ZONES OF CATION EXCHANGE'
0                         !nxtype= number of exchange zones
'zone          ex. capacity'
'-----------------------------------------------------------------------'
'end'
```

chemical.inp *

99    53    Read Ovr Block Sync Rec Caps

Figure 5-17.  Part of the TOUGHREACT input file, *chemical.inp*, for the sample problem discussed above: initial gas partial pressures and miscellaneous parameters.

**REFERENCES**

Alai, M., M. Sutton, and S. Carroll, 2005, Evaporative evolution of a Na–Cl–NO3–K–Ca–SO4–Mg–Si brine at 95 °C: Experiments and modeling relevant to Yucca Mountain, Nevada, GEOCHEMICAL TRANSACTIONS, 6 (2) 31-45.

Blowes, D. W., E. J. Reardon, J. L. Jambor, and J. A. Cherry, 1991, The formation and potential importance of cemented layers in inactive sulfide mine tailings, Geochim. Cosmochim. Acta, 55(4), 965-978.

Boufadel, M. C., M. T. Suidan, and A. D. Venosa, 1999, A numerical model for density-and-viscosity-dependent flows in two-dimensional variably saturated porous media, J. Contam. Hydrol., 37(1), 1-20.

Dougherty, R. C., 2001, Density of salt solution: Effects of ions on the apparent density of water, j. phys. Chem. B, 105(19), 4514-4519.

Felmy, A. R., H. Cho, J. R. Rustad, and M. J. Mason, 2001, An aqueous thermodynamic model for polymerized silica species to high ionic strength, J. Solution Chem., 30(6), 509–525.

Gephart, R. E., and R. E. Lundgren, 1998, Hanford Tank Cleanup, Battelle, Columbus, OH.

Gerson, A. R., and K. Zheng, 1997, Bayer process plant scale: Transformation of sodalite to cancrinite, J. Cryst. Growth, 171(1-2), 209-218.

Harvie, C.E. and Weare, J.H., 1980, The Prediction of Mineral Solubilities in Natural Waters: The Na–K–Mg–Ca–Cl–SO$_4$–H$_2$O System from Zero to High Concentration at 25°C, Geochimica et Cosmochimica Acta, 44, ((7)), 981-997, New York, New York, Pergamon Press.

Harvie, C.E., Moller, N., and Weare, J.H. 1984. The Prediction of Mineral Solubilities in Natural Waters: The Na-K-Mg-Ca-H-Cl-SO$_4$-OH-HCO$_3$-CO$_3$-H$_2$O System to High Ionic Strengths at 25°C, Geochimica et Cosmochimica Acta, 48, (4), 723-751. New York, New York: Pergamon Press.

Krumgalz, B. S. 2001, Application of the Pitzer ion-interaction model to natural hypersaline brines, J. Mol. Liq., 91(1), 3 –19.

Lichtner, P. C., 2001, FLOTRAN user manual, LA-UR-01-2349, Los Alamos national Laboratory, Los Alamos, New Mexico.

Lichtner, P. C., and A. Felmy, 2003, Estimation of Hanford SX tank waste compositions from historically derived inventories, Comput. Geosci.,29(3), 371– 383.

Lichtner, P. C., S. Yabusaki, K. Pruess, and C. I. Steefel, 2004, Role of competitive cation exchange on chromatographic displacement of cesium in the vadose zone beneath the Hanford S/SX tank farm, Vadose Zone J.,3(1), 203– 219.

Monnin, C., 1994, Density calculation and concentration scale conversions for natural waters, Comput. Geosci., 20 (10), 1435-1445.

Oldenburg, C. M., and K. Pruess, 1995, Dispersive transport dynamics in a strongly coupled groundwater-brine flow system, Water Resour. Res., 31(2), 289-302.

Park H., and P. Englezos, 1999, Thermodynamic modeling of sodium aluminosilicate formation in aqueous alkaline solutions, Ind. Eng. Chem. Res., 38(12), 4959-4965.

Pitzer, K. S. 1973, Thermodynamics of electrolytes, I. Theoretical basis and general equations, J. Phys. Chem., 77, 268– 277.

Pitzer, K.S., and G. Mayorga, 1973. Thermodynamics of electrolytes. II. Activity and osmotic coefficients for strong electrolytes with one or both ions univalent. J. Phys. Chem., 77, 2300-2307.

Pitzer, K.S. 1991. Ion Interaction Approach: Theory and Data Correlation, Chapter 3 of Activity Coefficients in Electrolyte Solutions, 2nd Edition, Pitzer, K.S., ed. Boca Raton, Florida: CRC Press, TIC: 251799.

Plummer, L. N., D. L. Parkhurst, G. W. Fleming, and S. A. Dunkle, 1988, A computer program incorporating Pitzer's equations for calculation of geochemical reactions in brines, U.S. Geol. Surv. Water Resour. Invest. Rep., 88-4153, 310 pp.

Pruess, K., 1991, TOUGH2 – A General-Purpose Numerical Simulator for Multiphase Fluid and Heat Flow, Report LBL-29400. Berkeley, California: Lawrence Berkeley Laboratory. ACC: NNA.19940202.0088.

Pruess, K., C. Oldenburg, and G. Moridis, 1999, TOUGH2 User's Guide, Version 2.0, LBNL 43134, Lawrence Berkeley National Laboratory, Berkeley, California. TIC: 253038.

Rard J. A., Wijesinghe, A.M., 2003, Conversion of parameters between different variants of Pitzer's ion-interaction model, both with and without ionic strength dependent higher-order terms. J. Chem. Thermodynamics, 35, 439-473.

Risacher, F., and A. Clement, 2001, A computer program for simulation of evaporation of natural waters to high concentration, Comput. Geosci., 27(2), 191–201.

Rogers, P. S. Z. Ph.D dissertation, Earth Sciences Division, University of California, Berkeley, CA, March, 1981.

Simunek, J., and Suares, D. L., 1994, Two-dimensional transport model for variably saturated porous media with major ion chemistry, Water Resour. Res., v. 30, p. 1115-1133, TIC: 240807

Sonnenthal, E. L., Spycher, N., 2001, Drift-Scale coupled processes (DST and THC seepage) models. AMR N0120/U0110 Rev.01, Yucca Mountain Project, Lawrence Berkeley National Laboratory, Berkeley, California, MOL.20010314.0003.

Sonnenthal E., A. Ito, N. Spycher, M. Yui, J. Apps, Y. Sugita, M. Conrad, and S. Kawakami, 2005. Approaches to modeling coupled thermal, hydrological, and chemical processes In the Drift Scale Heater Test at Yucca Mountain. *International Journal of Rock Mechanics and Mining Sciences, 42, 698-719.*

Spycher N. F., Sonnenthal, E. L., and Apps, J. A., 2003, Fluid flow and reactive transport around potential nuclear waste emplacement tunnels at Yucca Mountain, Nevada, J. of Contam. Hydrol., v.62-63, p. 653-673, TIC: 254205

Steefel, C. I., S. Carroll, P. Zhao, and S. Roberts, 2003, Cesium migration in Hanford sediment: A multisite cation exchange model based on laboratory transport experiment, J. Contam. Hydrol., 67(1–4), 219–246

van Gaans, P. F. M., and R. D. Schuiling, 1997, The waste sulfuric acid lake of the $TiO_2$-plant at Armyansk, Crimea, Ukraine, II. Modeling the chemical evolution with PHRQPITZ, Appl. Geochem., 12(2), 187-201.

Voss, C. I., and W. R. Souza, 1987, Variable density flow and solute transport simulation of regional aquifers containing a narrow freshwater-saltwater transition zone, Water Resour. Res., 23, 1851– 1866.

Wagner, W. and A. Pruβ, 2002, The IAPW formulation 1995 for the thermodynamic properties of ordi-nary water substance for general scientific use, *Jour. Phys. Ref. Data, 31*, 387-535.

Wolery T. J., and S. A. Daveler, 1992, EQ6, A Computer program for Reaction Path Modeling of Aqueous Geochemical System: Theoretical Manual, User's Guide, and Related Documentation (version 7.0), Lawrence Livermore National Laboratory.

Wolery, T.J. and Jarek, R.L. (2003). EQ3/6, Version 8.0, Software User's Manual, Software Document Number 10813-UM-8.0-00, *U.S. Department of Energy*, Office of Civilian Radioactive Waste Management, Office of Repository Development, 1261 Town Center Drive, Las Vegas, Nevada 89144, 2003.

Wolery T., Jove-Colon C., Rard., J., Wijesinghe., A., 2004, Pitzer Database Development: Description of the Pitzer Geochemical Thermodynamic Database data0.ypf. Appendix I in In-Drift Precipitates/Salts Model (P. Mariner) Report ANL-EBS-MD-000045 REV 02. Las Vegas, Nevada: Bechtel SAIC Company.

Xu, T., Sonnenthal E., Spycher N., and Prues K., 2005, TOUGHREACT Users'Guide: A Simulation Program for Non-isothermal Multiphase Reactive Geochemical Transport in Variably Saturated Geologic Media.

Xu, T., and Pruess, K, 1998, Coupled modeling of non-isothermal multiphase flow, solute transport and reactive chemistry in porous and fractured media: 1. Model development and validation, Lawrence Berkeley National Laboratory Report LBNL-42050, Berkeley, California, 38 pp. TIC: 243735.

Zhang,G. Z. Zheng, and J. Wang, 2005, Modeling reactive geochemical of concentrated aqueous solutions, Water Resour. Res., 41, W02018, doi: 10.1029/2004WR003097.

## APPENDIX A.  IMPLEMENTED  PITZER ION-INTERACTION MODEL

### A.1  FORMULATION OF THE PIZTER ION-INTERACTION MODEL

A generally accepted form of the Pitzer model was formulated in Harvie et al. (1984) and called the HMW formulation (model). This model has been implemented in TOUGREACT. In the HMW model, water activity is formulated as:

$$Ln(a_{H_2o}) = -\frac{m_w}{1000}(\sum_{i=1}^{N} m_i)\phi \tag{A1}$$

where $a_{H_2o}$ is water activity, $m_i$ is molality of species $i$, $m_w$ is molecular weight of water, $N$ is the number of species in the system, and $\phi$ is the osmotic coefficient, defined as:

$$
\begin{aligned}
\sum_{i=1}^{N} m_i(\phi-1) &= 2(-\frac{A^{\Phi}I^{\frac{3}{2}}}{1+1.2\sqrt{I}}) \\
&+ \sum_{c=1}^{N_c}\sum_{a=1}^{N_a} m_c m_a (B_{ca}^{\Phi} + ZC_{ca}) \\
&+ \sum_{c}\sum_{c'=c+1} m_c m_{c'}(\Phi_{cc'}^{\phi} + \sum_{a=1} m_a \psi_{cc'a}) \\
&+ \sum_{a}\sum_{a'=a+1} m_a m_{a'}(\Phi_{aa'}^{\phi} + \sum_{c=1} m_c \psi_{aa'c}) \\
&+ \sum_{n=1}^{N_n}\sum_{c=1}^{N_c} m_n m_c \lambda_{nc} + \sum_{n=1}^{N_n}\sum_{a=1}^{N_a} m_n m_a \lambda_{na} \\
&+ \sum_{n=1}^{N_n}\sum_{c=1}^{N_c}\sum_{a=1}^{N_a} m_n m_c m_a \zeta_{nca}
\end{aligned}
\tag{A2}
$$

where $I$ is the ionic strength, defined as $I = \frac{1}{2}\sum_{k=1}^{N} z_k^2 m_k$, and $z_k$ is the electrical charge of species $k$. The subscripts $c$, $a$, and $n$ denote cations, anions, and neutral species, respectively. The activity coefficients of cations ($\gamma_M$), anions ($\gamma_X$), and neutral species ($\gamma_N$) are respectively calculated as:

$$\ln \gamma_M = Z_M^2 F + \sum_{a=1}^{N_a} m_a (2B_{Ma} + ZC_{Ma})$$
$$+ \sum_{c=1} m_c (2\Phi_{Mc} + \sum_{a=1} m_a \psi_{Mca})$$
$$+ \sum_a \sum_{a'=a+1} m_a m_{a'} \psi_{aa'M} \qquad (A3)$$
$$+ |Z_M| \sum_{c=1}^{N_c} \sum_{a=1}^{N_a} m_c m_a C_{ca}$$
$$+ 2\sum_{n=1}^{N_n} m_n \lambda_{nM}$$

$$\ln \gamma_X = Z_X^2 F + \sum_{c=1}^{N_c} m_c (2B_{cX} + ZC_{cX})$$
$$+ \sum_{a=1} m_a (2\Phi_{Xa} + \sum_{c=1} m_c \psi_{Xac})$$
$$+ \sum_c \sum_{c'=c+1} m_c m_{c'} \psi_{cc'X} \qquad (A4)$$
$$+ |Z_x| \sum_{c=1}^{N_c} \sum_{a=1}^{N_a} m_c m_a C_{ca}$$
$$+ 2\sum_{n=1}^{N_n} m_n \lambda_{nX}$$

$$\ln \gamma_N = \sum_{a=1}^{N_a} m_a (2\lambda_{na}) + \sum_{c=1}^{N_c} m_c (2\lambda_{nc})$$
$$+ \sum_{c=1}^{N_c} \sum_{a=1}^{N_a} m_c m_a \zeta_{Nca} \qquad (A5)$$

where *F* is given by:

$$F = -A^\Phi \left( \frac{\sqrt{I}}{1+1.2\sqrt{I}} + \frac{2}{1.2} ln(1+1.2\sqrt{I}) \right)$$
$$+ \sum_{c=1} \sum_{c'=c+1} m_c m_{c'} \Phi'_{cc'} + \sum_{a=1} \sum_{a'=a+1} m_a m_{a'} \Phi'_{aa'} \qquad (A6)$$
$$+ \sum_{c=1}^{N_c} \sum_{a=1}^{N_a} m_c m_a B'_{ca}$$

$C_{MX}$ is derived from $C_{MX}^\Phi$ as:

$$C_{MX} = \frac{C_{MX}^\Phi}{2\sqrt{|z_M z_X|}} \qquad (A7)$$

and *Z* is calculated as:

$$Z = \sum_{k=1}^{N} |z_k| m_k \tag{A8}$$

The Pitzer virial coefficients, $B_{MX}^{\Phi}$, $B_{MX}$, $B_{MX}^{'}$, $\alpha_{MX}$, $C_{MX}$, $\lambda_{NC}$ and $\lambda_{NA}$ in Equation (A2) through (A7) are described below.

$B_{MX}^{\Phi}$, used to calculate the osmotic coefficient and water activity, is defined according to:

$$B_{MX}^{\Phi} = \beta_{MX}^{(0)} + \beta_{MX}^{(1)} e^{-\alpha_{MX}\sqrt{I}} + \beta_{MX}^{(2)} e^{-\alpha_{MX}^{'}\sqrt{I}} \tag{A9}$$

where $\beta_{MX}^{(0)}$, $\beta_{MX}^{(1)}$, $\beta_{MX}^{(2)}$, and $\alpha_{MX}$ are temperature-dependent ion-interaction parameters.

$B_{MX}$ is used to calculate the activity coefficient of charged species (ions). This coefficient is calculated as:

$$B_{MX} = \beta_{MX}^{(0)} + \beta_{MX}^{(1)} g(\alpha_{MX}\sqrt{I}) + \beta_{MX}^{(2)} g(\alpha_{MX}^{'}\sqrt{I}) \tag{A10}$$

with function g(x) defined as:

$$g(x) = 2(1 - (1 + x)e^{-x}) / x^2 \tag{A11}$$

and x denoting $\alpha_{MX}\sqrt{I}$ or $\alpha_{MX}^{'}\sqrt{I}$, respectively.

$B_{MX}^{'}$ is used to calculate the modified Debye-Hückel term, and is formulated as:

$$
\begin{aligned}
B_{MX}^{'} &= \frac{\partial B_{MX}}{\partial I} \\
&= \beta_{MX}^{(1)} \frac{g'(\alpha_{MX}\sqrt{I})}{I} + \beta_{MX}^{(2)} \frac{g'(\alpha_{MX}^{'}\sqrt{I})}{I}
\end{aligned} \tag{A12}
$$

with function $g^{'}(x)$ defined as:

$$g'(x) = -2(1 - (1 + x + \frac{x^2}{2})e^{-x}) / x^2 \tag{A13}$$

and x denoting $\alpha_{MX}\sqrt{I}$ or $\alpha_{MX}^{'}\sqrt{I}$, respectively.

For any salt containing a monovalent ion, $\alpha_{MX} = 2$ and $\alpha_{MX}^{'} = 12$; for 2-2 electrolytes, $\alpha_{MX} = 1.4$ and $\alpha_{MX}^{'} = 12$; for 3-2, 4-2, and higher valence electrolytes, $\alpha_{MX} = 2.0$ and $\alpha_{MX}^{'} = 50$.

Note that $\varPhi_{cc}^{\phi}$, $\varPhi_{aa}^{\phi}$, $\varPhi_{cc}$, $\varPhi_{aa}$, $\varPhi_{cc}^{'}$, $\varPhi_{aa}^{'}$ are interaction parameters for like-sign ionic pairs (mixing terms). They are temperature and ionic strength dependent:

$$\varPhi_{ij}^{\phi} = \theta_{ij} + {}^{E}\theta_{ij}(I) + I {}^{E}\theta_{ij}^{'}(I) \tag{A14}$$

$$\varPhi_{ij} = \theta_{ij} + {}^{E}\theta_{ij}(I) \tag{A15}$$

$$\varPhi_{ij}^{'} = {}^{E}\theta_{ij}^{'}(I) \tag{A16}$$

Terms ${}^{E}\theta_{ij}(I)$ and ${}^{E}\theta_{ij}^{'}(I)$ are functions of the ionic charges between the pair and solution ionic strength. These functions are defined in Pitzer (1991) and can normally be ignored in moderately concentrated solutions of ionic strength less than 10 molal (for all like-sign pairs, ${}^{E}\theta_{ij}(I) = 0$ and ${}^{E}\theta_{ij}^{'}(I) = 0$ ). Also, $\theta_{ij}$ are temperature-dependent fitting parameters, with ${}^{E}\theta_{ij}(I)$ and ${}^{E}\theta_{ij}^{'}(I)$ calculated according to Pitzer (1991). $\varPsi_{cca}$ and $\varPsi_{caa}$ are the temperature dependent interaction coefficients of ternary terms. $\zeta_{nca}$ is the temperature dependent interaction coefficient of neutral-cation-anion terms. Normally, this term is ignored (for all neutral-cation-anion triplets, $\zeta = 0$ ).

## A.2    SIMPLIFICATIONS OF THE PIZER MODEL IMPLEMENTED IN TOUGHREACT

When the Pitzer model is used in geochemical simulations, the calculation of ionic interactions can be computationally intensive. For reactive transport problems, calculations of ionic interaction make the simulation intensive and time consuming. On the other hand, a complete expression of the Piztzer's ionic interaction theory would need infinite interaction terms in the virial equation. Any explicit expression of the model, including those in Pitzer's orginal formulations and the HMW model, is just a simplified representation of the Pitzer's ionic interaction theory. Different levels of simplifications can be applied to solutions with different levels of ionic strength, without significant loss of accuracy. These simplifications can reduce the computational resources requirement and lead to a significant computational time saving. TOUGHREACT provides four different levels of simplification based on the standard HMW model. If MOPR(10) and MOPR(11) are set to 0, TOUGHREACT runs a full implementation of the HMW model (Eqs. A1 though A16). Simplifications are performed by assigning non-zero values to MOPR(10) and MOPR(11) as described below:

### A.2.1    Simplification 1, MOPR (11)=1

This setup neglects the ionic strength dependence of the mixing terms. With this setup, Equation (A14), (A15), and (A16) reduce to:

$$\varPhi_{ij}^{\phi} = \theta_{ij} \tag{A17}$$

$$\Phi_{ij} = \theta_{ij} \tag{A18}$$

$$\Phi'_{ij} = 0 \tag{A19}$$

No changes in other equations are made. This simplification is not recommended for use when dealing with solutions having an ionic strength higher than 10 molal.

### A.2.2    Simplification 2, MOPR(10)=1

This setup neglects the neutral-cation-anion terms (the last term) in Equations (A2) and (A5). These equations are then reduced to:

$$
\begin{aligned}
\sum_{i=1}^{N} m_i(\phi - 1) = {} & 2(-\frac{A^{\Phi}I^{\frac{3}{2}}}{1+1.2\sqrt{I}}) + \sum_{c=1}^{N_c}\sum_{a=1}^{N_a} m_c m_a( B_{ca}^{\Phi} + ZC_{ca} ) \\
& + \sum_{c}\sum_{c'=c+1} m_c m_{c'}( \Phi_{cc'}^{\phi} + \sum_{a=1} m_a \psi_{cc'a} ) \\
& + \sum_{a}\sum_{a'=a+1} m_a m_{a'}( \Phi_{aa'}^{\phi} + \sum_{c=1} m_c \psi_{aa'c} ) \\
& + \sum_{n=1}^{N_n}\sum_{c=1}^{N_c} m_n m_c \lambda_{nc} + \sum_{n=1}^{N_n}\sum_{a=1}^{N_a} m_n m_a \lambda_{na}
\end{aligned} \tag{A20}
$$

and

$$ \ln\gamma_N = \sum_{a=1}^{N_a} m_a( 2\lambda_{na} ) + \sum_{c=1}^{N_c} m_c( 2\lambda_{nc} ) \tag{A21}$$

Other equations are unchanged. This simplification generally yields virtually the same results as the full formulations, because the neutral-cation-anion terms are typically insignificant.  In addition, the parameters of these terms are usually not available, making the full formulation perform like the simplified formulation.  Thus, this simplification can be used in most cases.

### A.2.3    Simplification 3, MOPR(10)=2

In addition to the terms neglected in Simplification 2, this option neglects the cation-cation-anion and the cation-anion-anion terms in Equation (A2), (A3), and (A4). These equations then reduce to:

$$
\begin{aligned}
\sum_{i=1}^{N} m_i(\phi - 1) = {} & 2(-\frac{A^{\Phi}I^{\frac{3}{2}}}{1+1.2\sqrt{I}}) + \sum_{c=1}^{N_c}\sum_{a=1}^{N_a} m_c m_a( B_{ca}^{\Phi} + ZC_{ca} ) \\
& + \sum_{c}\sum_{c'=c+1} m_c m_{c'} \Phi_{cc'}^{\phi} + \sum_{a}\sum_{a'=a+1} m_a m_{a'} \Phi_{aa'}^{\phi} \\
& + \sum_{n=1}^{N_n}\sum_{c=1}^{N_c} m_n m_c \lambda_{nc} + \sum_{n=1}^{N_n}\sum_{a=1}^{N_a} m_n m_a \lambda_{na}
\end{aligned} \tag{A22}
$$

$$ln\,\gamma_M = Z_M^2 F + \sum_{a=1}^{N_a} m_a(\,2B_{Ma} + ZC_{Ma}\,)$$

$$+ 2\sum_{c=1}^{N_c} m_c \Phi_{Mc} + |Z_M| \sum_{c=1}^{N_c} \sum_{a=1}^{N_a} m_c m_a C_{ca} + 2\sum_{n=1}^{N_n} m_n \lambda_{nM} \tag{A23}$$

$$ln\,\gamma_X = Z_X^2 F + \sum_{c=1}^{N_c} m_c(\,2B_{cX} + ZC_{cX}\,)$$

$$+ 2\sum_{c=1}^{N_c} m_a \Phi_{Xa} + |Z_x| \sum_{c=1}^{N_c} \sum_{a=1}^{N_a} m_c m_a C_{ca} + 2\sum_{n=1}^{N_n} m_n \lambda_{nX} \tag{A24}$$

This simplification can be generally used for solutions with an ionic strength smaller than about 10 molal.

### A.2.4 Simplification 4, MOPR(10)=3

In addition to the terms neglected in Simplification 3, this setup neglects cation-cation and anion-anion terms in Equations (A2), (A3), and (A4), which reduce to:

$$\sum_{i=1}^{N} m_i(\,\phi - 1\,) = 2(-\frac{A^{\Phi} I^{\frac{3}{2}}}{1 + 1.2\sqrt{I}}) + \sum_{c=1}^{N_c} \sum_{a=1}^{N_a} m_c m_a(\,B_{ca}^{\Phi} + ZC_{ca}\,)$$

$$+ \sum_{n=1}^{N_n} \sum_{c=1}^{N_c} m_n m_c \lambda_{nc} + \sum_{n=1}^{N_n} \sum_{a=1}^{N_a} m_n m_a \lambda_{na} \tag{A25}$$

$$ln\,\gamma_M = Z_M^2 F + \sum_{a=1}^{N_a} m_a(\,2B_{Ma} + ZC_{Ma}\,) + |Z_M| \sum_{c=1}^{N_c} \sum_{a=1}^{N_a} m_c m_a C_{ca} + 2\sum_{n=1}^{N_n} m_n \lambda_{nM} \tag{A26}$$

$$ln\,\gamma_X = Z_X^2 F + \sum_{c=1}^{N_c} m_c(\,2B_{cX} + ZC_{cX}\,) + |Z_x| \sum_{c=1}^{N_c} \sum_{a=1}^{N_a} m_c m_a C_{ca} + 2\sum_{n=1}^{N_n} m_n \lambda_{nX} \tag{A27}$$

This simplification can be generally used for solutions with an ionic strength smaller than 5 molal.

Note that the use of the full version of the formulation (no simplification) usually yields better results if all interaction parameters are available and self-consistent; in this case, simplification is not encouraged if computational power is not limited. Note also that because interaction parameters are typically obtained by fitting experimental data using some level of simplification in the HMW formulation, the user should be careful to set a simplification level that matches (as well as possible) the formulation used to fit the experimental data.